AIMS Mathematics

http://www.aimspress.com/journal/Math

AIMS Mathematics, 11(8): 24877–24912.
DOI: 10.3934/math.20261000
Received: 03 June 2026
Revised: 02 August 2026
Accepted: 07 August 2026
Published: 13 August 2026

Research article

A kernel regression-based hybrid forecasting framework for highly volatile energy commodity markets

Hasnain Iftikhar[1,*], Said Farooq Shah[1], Fatimah E. Almuhayfith[2,*] and Paulo Canas Rodrigues[3,4]

[1] Department of Statistics, University of Peshawar, Peshawar, Pakistan
[2] Department of Mathematics and Statistics, College of Science, King Faisal University, Alahsa 31982, Saudi Arabia
[3] Department of Statistics, Federal University of Bahia, Salvador 40170-110, Brazil
[4] Department of Business Management, University of Pretoria, Pretoria 0002, South Africa

* **Correspondence:** Email: hasnain.iftikhar@uop.edu.pk, falmuhaifeez@kfu.edu.sa.

Abstract: In today's energy markets, forecasting energy commodity prices is difficult due to pronounced nonlinearity, nonstationarity, volatility clustering, structural changes, and multi-scale temporal dependencies. These features are of significant importance for financial risk management, portfolio allocation, derivative pricing, and decision-making in energy markets. To address these problems, we proposed a novel hybrid forecasting framework that combines a decomposition method based on kernel regression and nonparametric kernel smoothing with linear and nonlinear forecasting models. The proposed approach decomposes each energy commodity price into a smooth trend component and a stochastic fluctuation component. This enables the long-run market trend to be modeled separately from short-run fluctuations and localized market variability. The proposed framework was evaluated using five major global energy commodity markets, including WTI crude oil, Brent crude oil, natural gas, gasoline, and heating oil. Empirical results demonstrate that the proposed decomposition-based method consistently outperforms the best forecasting models proposed in the literature, direct hybrid models, and traditional standalone forecasting models across multiple statistical measures and tests of accuracy and efficiency. Our results indicated that kernel-based decomposition effectively captures complex nonlinear dependence structures while separating persistent trends from short-run fluctuations, leading to significant improvements in forecasting accuracy, forecast stability, and directional forecasting performance. The results indicated that the proposed framework can serve as a reliable tool for energy market forecasting and financial analytics to model and predict highly volatile commodity markets and other complex financial time series.

Keywords: energy commodity markets; nonparametric kernel regression; financial data analytics;

hybrid forecasting models; mathematical finance
Mathematics Subject Classification: 62M10, 62M20, 62G08, 91G70, 91B84

1. Introduction

West Texas Intermediate (WTI) crude oil, Brent crude oil, natural gas (NATGAS), gasoline (GASOLINE), and heating oil (HEATOIL) are major energy commodities that play a central role in global production, transportation, electricity generation, and industrial activity [1–5]. Their prices directly influence inflation, economic growth, financial markets, and energy security, making accurate forecasting essential for both policy and investment decisions [6]. Energy markets have experienced substantial volatility due to geopolitical conflicts, economic uncertainty, supply-chain disruptions, climate-related events, and structural changes in global energy systems [7–11]. Consequently, energy prices exhibit nonlinear, nonstationary, and regime-dependent behavior with frequent structural breaks. Although individual commodities are driven by different market-specific factors, their prices remain strongly interconnected, making accurate forecasting both economically important and statistically challenging [12–16].

Accurate forecasting of energy prices is of crucial importance for governments, policymakers, investors, financial institutions, and energy producers [17–20]. It is also useful for energy policymaking, monetary planning, inventory management, portfolio optimization, derivative pricing, hedging strategy, and energy trading systems [21–24]. However, the forecasting performance is often limited by the nonlinear, nonstationary, heteroscedastic, and chaotic properties of energy time series [25–28]. Traditional statistical and econometric approaches have been widely used for energy forecasting, such as autoregressive, autoregressive moving average, autoregressive integrated moving average, generalized autoregressive conditional heteroscedasticity, and vector autoregression [29–32]. While these methods work well in relatively stable market conditions, their forecasting ability often degrades under nonlinear dynamics and rapidly changing volatility structures. To overcome these limitations, attention has shifted toward machine learning and non-linear forecasting models [33]. On the other hand, forecasting studies have compared alternative regression-based approaches for improving predictive accuracy in economic applications [34]. Methods such as support vector regression, artificial neural networks, nonparametric autoregressive models, and long short-term memory models have shown improved ability to capture nonlinear temporal structures and hidden stochastic dependencies in energy price series [35–39]. However, standalone machine learning models may still be subject to overfitting, instability, and a lack of interpretability when applied to highly noisy and nonstationary datasets [40]. Moreover, decomposition-based hybrid forecasting frameworks have emerged as powerful tools to model complex financial and energy time series [41, 42]. In the first step, these frameworks decompose the original series into simpler subcomponents and then apply forecasting models to each subcomponent separately. Signal decomposition methods like wavelet transform [43], empirical mode decomposition [44–46], variational mode decomposition [47, 48], singular spectrum analysis [49–51], and complete ensemble empirical mode decomposition with adaptive noise [52] have achieved significant improvement of forecasting performance by reducing the signal complexity and enhancing the hidden pattern extraction [53–56]. However, decomposition methods are limited by mode mixing, parameter sensitivity, computational instability, and limited adaptability to fast-changing market conditions. Existing decomposition methods are also limited by mode mixing, parameter sensitivity, computational instability, and limited adaptability to fast-changing market conditions. In contrast, the proposed kernel regression-based decomposition estimates the underlying trend directly through nonparametric local smoothing rather than iterative mode extraction or frequency-domain decomposition. This enables the framework to flexibly adapt to local market dynamics while avoiding decomposition artifacts associated with empirical mode decomposition techniques. Furthermore, by combining multiple kernel functions with component-wise hybrid forecasting models, we propose framework provides a flexible and computationally efficient approach for modeling nonlinear dynamics and stochastic volatility patterns in energy commodity markets.

Motivated by these limitations, we proposed a kernel regression-based decomposition framework that decomposes energy price series into smooth trend and fluctuation components using four kernel functions, namely Gaussian, Truncated Gaussian, Uniform, and Epanechnikov kernels. Linear (AR and ARIMA) and nonlinear (NPAR and NNAR) forecasting models are then applied to each component individually before reconstructing the final forecasts. The major contributions of this study are fourfold. First, we develop a nonparametric kernel regression-based decomposition approach for forecasting energy commodity price series exhibiting high volatility, nonlinear dynamics, and structural heterogeneity. Rather than explicitly modeling a latent volatility process or forecasting conditional variance, the proposed framework adaptively separates long-run market movements from short-run fluctuations, thereby facilitating more effective component-wise forecasting of highly volatile energy prices. Second, we propose a hybrid forecasting framework that incorporates linear and nonlinear forecasting models to harness the unique statistical characteristics of the decomposed trend and fluctuation components. Third, we develop the theoretical properties of the proposed framework, such as variance reduction and asymptotic consistency, which provide rigorous statistical justifications for the proposed decomposition-based forecasting methodology. Fourth, we perform extensive empirical experiments on five major global energy commodity markets using different forecasting accuracy measures, directional statistics, efficiency metrics, and statistical significance tests to show the effectiveness, robustness, and statistical superiority of the proposed methodology.

The rest of the paper is structured as follows: In Section 2 we describes the proposed nonparametric decomposition methodology and hybrid forecasting framework. In Section 3, we cover the data, empirical design, and forecasting results. A detailed discussion on comparative analyses and future research directions is given in Section 4. Finally, in Section 5 we conclude this study.

2. The proposed kernel regression-based decomposition framework

In this paper, we propose a nonparametric kernel regression based decomposition and hybrid forecasting approach for highly volatile energy commodity markets including West Texas Intermediate (WTI) crude oil, Brent crude oil, natural gas (NATGAS), gasoline (GASOLINE) and heating oil (HEATOIL). Energy commodity prices display characteristics of non-linear dependence, non-stationarity, volatility clustering, heavy-tailed distributions, structural breaks, and regime dependent dynamics, which are difficult to handle with traditional approaches to forecasting. Mathematically, the price series can be viewed as realizations of complex stochastic processes, which are driven by persistent long-run forces and rapidly evolving short-run fluctuations in the market. The proposed approach differs from classical stochastic volatility or GARCH-type models that explicitly model the latent conditional variance. It uses kernel regression to decompose the observed price series into a smooth trend component and a fluctuation component. The trend reflects persistent long-run market dynamics associated with macroeconomic fundamentals and structural conditions. The fluctuation component retains short-run nonlinear dynamics, volatility clustering, and sudden market movements. The individual components are then modeled separately with linear and non-linear forecasting models, which are additively recombined to form the final forecast. The proposed methodology does not provide an explicit parametric volatility model but exploits the different statistical properties of the decomposed components. It offers a flexible, robust, and effective framework for predicting highly volatile energy commodity prices and thus contributes to financial data analytics for complex nonlinear markets.

2.1. Kernel regression-based decomposition technique

In this subsection, we elaborate on the proposed kernel regression-based decomposition technique for forecasting energy commodity price series. Let $\left\{Y_t^{(m)}\right\}_{t=1}^{N}$, $\quad m \in \mathcal{M} = \{1, 2, 3, 4, 5\}$, denote the observed daily energy commodity price series, where: $1 \rightarrow$ WTI crude oil, $2 \rightarrow$ Brent crude oil, $3 \rightarrow$ NATGAS, $4 \rightarrow$ GASOLINE, $5 \rightarrow$ HEATOIL. Here, t is the time index and N is the number of observations. The variable t is the time index for chronological ordering of daily observations of the market. We assume the observed financial time series contains both deterministic and stochastic parts. Accordingly, the proposed decomposition framework decomposes the observed energy commodity price into the additive combination of a long-run trend component and a short-run fluctuation component as follows:

$$Y_t^{(m)} = T_t^{(m)} + F_t^{(m)}, \qquad t = 1, 2, \ldots, N, \tag{2.1}$$

where $T_t^{(m)}$ is the smooth long-run trend component and $F_t^{(m)}$ is the short-run fluctuation component. The trend component captures long-term market movements attributed to economic growth, institutional investment behavior, and macroeconomic conditions, while the fluctuation component captures local irregularities, nonlinear stochastic dependence, speculative activity, and volatility dynamics. However, the decomposition in Eq (2.1) can be interpreted as a partition of low- and high-frequency information embedded in the dynamics of the observed price. This representation is particularly relevant in mathematical finance, where the prices of financial assets often exhibit heterogeneous time scales and volatility persistence.

The long-run trend component is estimated using a kernel regression smoother. Kernel regression is a nonparametric estimation technique that estimates the underlying trend structure without assuming a prior functional relationship between the response and the explanatory variables. Kernel regression can better model evolving market dynamics and nonlinear temporal structures than parametric trend estimation techniques because it can adapt flexibly to local data characteristics. The following is the kernel regression estimator for the trend component:

$$\widehat{T}_t^{(m)} = \sum_{s=1}^{N} w_{t,s}(h)\, Y_s^{(m)}, \tag{2.2}$$

where $w_{t,s}(h)$ denotes the normalized kernel weights defined as

$$w_{t,s}(h) = \frac{K\left(\frac{t-s}{h}\right)}{\sum_{j=1}^{N} K\left(\frac{t-j}{h}\right)}, \tag{2.3}$$

subject to the normalization condition

$$\sum_{s=1}^{N} w_{t,s}(h) = 1.$$

Equivalently, the trend estimator can be expressed as

$$\widehat{T}_t^{(m)} = \frac{\sum_{s=1}^{N} K\left(\frac{t-s}{h}\right) Y_s^{(m)}}{\sum_{s=1}^{N} K\left(\frac{t-s}{h}\right)}. \tag{2.4}$$

The kernel function is denoted by $K(\cdot)$ in the preceding formulation, and the bandwidth parameter that controls the degree of smoothness is represented by $h > 0$. Because it establishes the trade-off between bias and variance, the bandwidth parameter is essential to nonparametric estimation. Larger bandwidth values result in smoother trend estimates as they average over larger areas. Smaller bandwidth values maintain local fluctuations and nonlinearities because they put more weight on nearby observations. The choice of bandwidth is essential for capturing the underlying structures of the financial markets. The fluctuation component is obtained from the remainder of the observed series after subtracting the calculated trend component. The trend component is obtained as follows:

$$\widehat{F}_t^{(m)} = Y_t^{(m)} - \widehat{T}_t^{(m)}. \tag{2.5}$$

The fluctuation component contains high-frequency stochastic information, short-term volatility, irregular market movements, and nonlinear dependencies that cannot be explained by the long-run trend structure. Kernel regression performance depends heavily on the choice of kernel function. The decomposition accuracy depends on the smoothing properties of different kernel architectures. In this work, four kernel functions are used, namely Gaussian, Epanechnikov, Uniform, and reduced Gaussian, to capture different market dynamics and local temporal characteristics. The Gaussian kernel is

$$K(u) = \frac{1}{\sqrt{2\pi}} \exp\left(-\frac{u^2}{2}\right). \tag{2.6}$$

The Gaussian kernel down-weights observations as they are further away. This leads to infinitely smooth weighting. This property makes it very useful for evaluating persistent financial fluctuations and smooth long-term market structures. The Epanechnikov kernel is given by

$$K(u) = \frac{3}{4}(1 - u^2)\,\mathbb{I}(|u| \leq 1), \tag{2.7}$$

where the indicator function is denoted by $\mathbb{I}(\cdot)$. The Epanechnikov kernel is an efficient kernel for local smoothing because it achieves the best asymptotic efficiency in terms of mean integrated squared error. The Uniform kernel is defined by

$$K(u) = \frac{1}{2}\mathbb{I}(|u| \leq 1). \tag{2.8}$$

The Uniform kernel, in contrast to smooth kernels, assigns equal weight to each observation in the local neighborhood. A simple structure results in stable local averaging properties and computational efficiency. The truncated Gaussian kernel is given by

$$K(u) = \frac{\phi(u)}{\Phi(a) - \Phi(-a)} \mathbb{I}(|u| \leq a), \tag{2.9}$$

In the aforementioned formula, the parameter $a > 0$ serves as the truncation parameter, while $\phi(\cdot)$ and $\Phi(\cdot)$ denote the standard normal density and cumulative distribution functions, respectively. The truncated Gaussian kernel enhances robustness in volatile market conditions by maintaining the smooth weighting structure of the Gaussian kernel while diminishing the impact of extreme observations and tail effects.

2.2. *Theoretical foundation of the proposed hybrid framework*

While the proposed methodology combines kernel regression decomposition with linear and nonlinear forecasting models, its effectiveness can also be justified theoretically. The decomposition process reduces structural complexity by decomposing the original time series into smoother trend and stochastic fluctuation components, which enables forecasting models to learn more homogeneous temporal patterns. In this subsection, we describe the theoretical basis of the proposed framework.

2.2.1. Additive decomposition representation

Let the observed energy commodity price series be denoted as where

$$Y_t = m(t) + \varepsilon_t, \qquad t = 1, 2, \ldots, N, \tag{2.10}$$

where $m(t)$ denotes an unknown smooth trend function and $\{\varepsilon_t\}$ is assumed to be a strictly stationary, weakly dependent stochastic process satisfying standard α-mixing conditions with finite second moment $E(\varepsilon_t^2) < \infty$. Furthermore,

$$E(\varepsilon_t) = 0, \qquad 0 < \sigma_t^2 = \mathrm{Var}(\varepsilon_t) \leq C < \infty,$$

for some finite constant C. These assumptions enable moderate heteroscedasticity and serial dependence, which are commonly observed in financial and energy commodity price series. Using kernel regression, the trend component is estimated as $\widehat{T}_t = \widehat{m}(t)$, and the fluctuation component is obtained as $\widehat{F}_t = Y_t - \widehat{T}_t$. Hence, the original series is decomposed into $Y_t = \widehat{T}_t + \widehat{F}_t$. This decomposition enables separate modeling of the long-run deterministic behavior and the short-run stochastic dynamics.

2.2.2. Variance reduction property

The kernel estimator can be expressed as $\widehat{T}_t = \sum_{s=1}^{N} w_{t,s} Y_s$, where $\sum_{s=1}^{N} w_{t,s} = 1$.

Proposition 1. Suppose that $\{\varepsilon_t\}$ is a strictly stationary α-mixing process with finite second moments and bounded conditional variance satisfying

$$0 < \sigma_t^2 \leq C < \infty,$$

where C is a finite positive constant. Then the variance of the kernel-smoothed trend estimator satisfies

$$\mathrm{Var}(\widehat{T}_t) \leq C \sum_{s=1}^{N} w_{t,s}^2. \tag{2.11}$$

Since

$$\sum_{s=1}^{N} w_{t,s}^2 < 1, \tag{2.12}$$

for any non-degenerate kernel weighting scheme, it follows that

$$\mathrm{Var}(\widehat{T}_t) < \mathrm{Var}(Y_t). \tag{2.13}$$

Proof. Since the kernel estimator is a weighted average of weakly dependent observations,

$$\mathrm{Var}(\widehat{T}_t) = \sum_{i=1}^{N} \sum_{j=1}^{N} w_{t,i} w_{t,j} \,\mathrm{Cov}(Y_i, Y_j). \tag{2.14}$$

Under the assumed α-mixing condition with bounded second moments, the covariance terms decay sufficiently fast as the temporal lag increases. Consequently,

$$\mathrm{Var}(\widehat{T}_t) \leq C \sum_{s=1}^{N} w_{t,s}^2, \tag{2.15}$$

where

$$C = \sup_t \sigma_t^2 < \infty.$$

Because the kernel weights satisfy

$$\sum_{s=1}^{N} w_{t,s} = 1, \qquad \sum_{s=1}^{N} w_{t,s}^2 < 1,$$

it follows that

$$\mathrm{Var}(\widehat{T}_t) < C.$$

Hence, kernel smoothing reduces the variability of the observed process while preserving its underlying long-run trend. Thus, kernel regression produces a statistically smoother representation of the original series by reducing the influence of high-frequency stochastic fluctuations while preserving the underlying long-run dynamics. This variance reduction improves the signal-to-noise ratio,enabling the subsequent forecasting models to learn more homogeneous temporal structures and thereby enhancing forecasting accuracy and stability for highly volatile financial and energy commodity markets.

2.2.3. Forecast error decomposition

Let the reconstructed forecast be defined as

$$\widehat{Y}_{t+h} = \widehat{T}_{t+h} + \widehat{F}_{t+h}, \tag{2.16}$$

where $\widehat{T}_{t+h}$ and $\widehat{F}_{t+h}$ denote the forecasts of the trend and fluctuation components, respectively.

The forecast error can be written as

$$e_{t+h} = Y_{t+h} - \widehat{Y}_{t+h}. \tag{2.17}$$

Substituting the decomposition yields

$$e_{t+h} = \left(T_{t+h} - \widehat{T}_{t+h}\right) + \left(F_{t+h} - \widehat{F}_{t+h}\right). \tag{2.18}$$

Define

$$e_T = T_{t+h} - \widehat{T}_{t+h}, \tag{2.19}$$

and

$$e_F = F_{t+h} - \widehat{F}_{t+h}. \tag{2.20}$$

Then

$$e_{t+h} = e_T + e_F. \tag{2.21}$$

Consequently,

$$\mathrm{MSE}(e) = \mathrm{MSE}(e_T) + \mathrm{MSE}(e_F) + 2\ \mathrm{Cov}(e_T, e_F). \tag{2.22}$$

Since kernel regression separates the original series into low-frequency trend and high-frequency fluctuation components, their corresponding forecasting errors are expected to exhibit weak asymptotic dependence because kernel decomposition separates low-frequency and high-frequency dynamics. Under standard regularity conditions, then

$$\mathrm{Cov}(e_T, e_F) = o(1), \qquad N \to \infty,$$

which leads to

$$\mathrm{MSE}(e) = \mathrm{MSE}(e_T) + \mathrm{MSE}(e_F) + o(1),$$

where the covariance term becomes asymptotically negligible. This provides a stronger theoretical justification for component-wise forecasting without requiring exact independence between the two forecasting errors.

2.2.4. Consistency of the proposed framework

The asymptotic behavior of the proposed hybrid forecasting framework can be established under standard regularity conditions for nonparametric kernel regression and consistent forecasting models.

Theorem 1. Suppose that the following conditions hold:

1. The stochastic process $\{Y_t\}$ is strictly stationary after removing the deterministic trend and satisfies standard α-mixing conditions with finite second moments.
2. The regression function $m(\cdot)$ is twice continuously differentiable on its support.
3. The kernel function satisfies
$$\int_{-\infty}^{\infty} K(u)\, du = 1, \tag{2.23}$$
$$K(u) = K(-u), \tag{2.24}$$
and
$$\int_{-\infty}^{\infty} u^2 K(u)\, du < \infty. \tag{2.25}$$
4. The bandwidth sequence satisfies
$$h \to 0, \qquad Nh \to \infty, \tag{2.26}$$
as $N \to \infty$.
5. The forecasting models applied to the trend and fluctuation components are statistically consistent, i.e., their prediction errors converge uniformly in probability.

Then the reconstructed hybrid forecast satisfies

$$\widehat{Y}_{t+h} \xrightarrow{p} Y_{t+h}, \qquad N \to \infty. \tag{2.27}$$

Proof. Under the standard regularity conditions for kernel regression, the kernel estimator is consistent, implying

$$\widehat{T}_t \xrightarrow{p} T_t. \tag{2.28}$$

Hence,

$$\widehat{F}_t = Y_t - \widehat{T}_t \xrightarrow{p} F_t. \tag{2.29}$$

Since the forecasting models for both decomposed components are assumed to be statistically consistent,

$$\widehat{T}_{t+h} \xrightarrow{p} T_{t+h}, \tag{2.30}$$

and

$$\widehat{F}_{t+h} \xrightarrow{p} F_{t+h}. \tag{2.31}$$

Applying Slutsky's theorem yields

$$\widehat{Y}_{t+h} = \widehat{T}_{t+h} + \widehat{F}_{t+h} \xrightarrow{p} Y_{t+h}. \tag{2.32}$$

Furthermore, under the finite second-moment assumption,

$$E\left[\left(\widehat{Y}_{t+h} - Y_{t+h}\right)^2\right] \longrightarrow 0, \qquad N \to \infty, \tag{2.33}$$

which establishes mean-square consistency of the proposed hybrid forecasting framework.

Therefore, the proposed decomposition-based forecasting framework is asymptotically consistent in a probability and mean-square sense. The kernel regression decomposition consistently estimates the latent trend component, while the component-wise forecasting models converge to the underlying data-generating process under the stated regularity conditions. Together, these results provide a rigorous statistical foundation for applying the proposed framework to nonlinear, weakly dependent stochastic volatility financial time series and hence justify its use in financial forecasting, portfolio optimization, risk management, and financial data analytics.

2.3. *Modeling the decomposed components*

After decomposition, the trend and fluctuation components are modeled independently using linear and nonlinear forecasting models, respectively. The component-wise approach enables the framework to capture diverse temporal structures better than directly modeling the original series. The fluctuation part includes local anomalies, volatility clustering, and nonlinear stochastic patterns. The trend component exhibits smoother, more consistent temporal dependence. This provides better predictability, adaptability, and interpretability. Thus, four standard forecasting models are used to model each component: Autoregressive, Autoregressive Moving Average, Nonparametric Autoregressive, and Neural Network Autoregressive.

2.3.1. Autoregressive model

One of the most basic linear stochastic time-series models is the autoregressive model [57]. It is predicated on the idea that this observation is linearly dependent on its prior values. For a component that is stationary

$$X_t^{(m)} \in \{T_t^{(m)}, F_t^{(m)}\},$$

the AR(p) process is defined as

$$X_t^{(m)} = \sum_{i=1}^{p} \phi_i X_{t-i}^{(m)} + \varepsilon_t^{(m)}, \tag{2.34}$$

where $\varepsilon_t^{(m)}$ represents a white-noise process with zero mean and constant variance, and ϕ_i are autoregressive coefficients. When simulating smooth temporal persistence and short-memory linear dependence in financial time series, the AR model excels.

2.3.2. Autoregressive moving average model

By adding moving-average variables that capture shock propagation and serial dependence in the innovation process, the ARMA model extends the AR framework [58]. The expression for the ARMA(p, q) model is

$$X_t^{(m)} = \sum_{i=1}^{p} \phi_i X_{t-i}^{(m)} + \varepsilon_t^{(m)} + \sum_{j=1}^{q} \theta_j \varepsilon_{t-j}^{(m)}, \tag{2.35}$$

where ϕ_i and θ_j denote autoregressive and moving average parameters, respectively. The ARMA model simultaneously captures persistence and shock-transmission dynamics, thereby providing greater flexibility in modeling financial market behavior.

2.3.3. Nonparametric autoregressive model

Linear models are computationally efficient and statistically interpretable, but they cannot explain the nonlinear temporal dependence in financial time series. The Nonparametric Autoregressive (NPAR) model overcomes this restriction [59]. The NPAR model overcomes assumptions of linearity by explicitly estimating unknown nonlinear functions from the data. The NPAR model is defined as

$$F_t^{(m)} = \sum_{i=1}^{p} f_i\left(F_{t-i}^{(m)}\right) + \varepsilon_t^{(m)}, \tag{2.36}$$

where $f_i(\cdot)$ are smooth unknown nonlinear functions estimated nonparametrically. The NPAR framework is highly flexible and can capture nonlinear dependence structures, asymmetric market behavior, and local stochastic variations.

2.3.4. Neural network autoregressive model

The proposed framework is enhanced further by incorporating the Neural Network Autoregressive (NNAR) model for better nonlinear forecasting capability [60]. The NNAR model is a universal function approximator and can learn very complex nonlinear relationships from historical observations. The NNAR(p, k) model for a component $X_t^{(m)}$ is defined as

$$X_t^{(m)} = \alpha_0 + \sum_{j=1}^{k} \alpha_j g\left(\beta_{j0} + \sum_{i=1}^{p} \beta_{ji} X_{t-i}^{(m)}\right) + \varepsilon_t^{(m)}, \tag{2.37}$$

where $g(\cdot)$ is a nonlinear activation function, k is the number of hidden neurons, and α_j and β_{ji} are neural network parameters. The NNAR model can capture the nonlinear interactions, volatility clustering, threshold effects, and higher-order temporal dependencies often observed in financial markets.

2.3.5. Model parameter selection

In this work, the forecasting models are estimated using automatic data-driven parameter selection procedures to ensure consistency, reproducibility, and objective model specification throughout the forecasting experiments. A summary of the software packages, parameter selection procedures, and implementation settings is provided in Table 1.

For the AR and ARIMA models, lag orders are selected automatically using the Akaike Information Criterion (AIC), while the ARIMA model additionally determines the required differencing order. The NPAR and NNAR models are implemented using the `tsDyn` [61] and `forecast` [62] packages in R, respectively, with their model orders selected automatically according to the default data-driven procedures of the corresponding packages. For NNAR, the number of hidden neurons is determined by the default rule $k = \left\lfloor \frac{p+1}{2} \right\rfloor$, where p denotes the selected autoregressive lag order.

For the proposed kernel regression decomposition, the bandwidth parameter is estimated automatically using the `np` package [63] based on least-squares cross-validation (LSCV). During the expanding-window forecasting experiment, the bandwidth and all forecasting model parameters are re-estimated at each forecasting origin using only the information available up to that time, thereby preventing information leakage and ensuring a fair out-of-sample evaluation. The Gaussian, Epanechnikov, Uniform, and Truncated Gaussian kernels employ the default implementations provided by the `np` package, while the Truncated Gaussian kernel uses the default second-order specification throughout all experiments. These automated parameter selection procedures minimize subjective tuning, reduce the risk of overfitting, and ensure reproducible comparisons among all competing forecasting models.

Table 1. Summary of software packages, parameter selection procedures, and implementation settings used in the forecasting framework.

Component	Software/Package	Parameter Selection	Setting
AR	`forecast`	Lag order selected using AIC	Re-estimated at each expanding window
ARIMA	`forecast`	Orders (p, d, q) selected using AIC	Re-estimated at each expanding window
NPAR	`tsDyn`	Automatic model order and smoothing parameter selection	Re-estimated at each expanding window
NNAR	`forecast`	Automatic lag selection; hidden nodes determined by $k = \lfloor (p+1)/2 \rfloor$	Re-estimated at each expanding window
Kernel bandwidth	`np`	Least-squares cross-validation (LSCV)	Re-estimated at each expanding window
Gaussian kernel	`np`	Standard kernel implementation	Default package specification
Epanechnikov kernel	`np`	Standard kernel implementation	Default package specification
Uniform kernel	`np`	Standard kernel implementation	Default package specification
Truncated Gaussian kernel	`np`	Default second-order truncated Gaussian implementation	Default package specification

In this work, a uniform notation system is introduced for all hybrid kernel regression-based forecasting models to provide a more systematic, comprehensible, and scalable representation of the proposed forecasting structures. The kernel-based decomposition technique, the forecasting model for the trend component, and the forecasting model for the fluctuation component are the three major components of the framework integrated into the suggested notation. However, all possible hybrid forecasting structures developed in this study can be efficiently categorized and interpreted using this organized mathematical representation. The generalized representation of the proposed hybrid forecasting framework is mathematically expressed as $\mathbb{H}_K^{(X \to Y)}$, where the subscript K denotes the kernel-based decomposition method, while the superscript pair $(X \to Y)$ identifies the forecasting models used for the trend and fluctuation components, respectively. Under this framework, the final forecast is obtained through the additive reconstruction of the independently forecasted components and is defined as

$$\widehat{Y}_{t+h} = \widehat{T}^{(X)}_{t+h} + \widehat{F}^{(Y)}_{t+h}, \tag{2.38}$$

where $\widehat{T}^{(X)}_{t+h}$ denotes the h-step-ahead forecast of the trend component generated using forecasting model X, and $\widehat{F}^{(Y)}_{t+h}$ represents the corresponding forecast of the fluctuation component obtained from forecasting model Y. For example, the notation $\mathbb{H}_G^{(I\to A)}$ represents a hybrid forecasting structure in which the Gaussian kernel decomposition method is employed, the trend component is modeled using the ARIMA model, and the fluctuation component is modeled using the AR model. Similarly, $\mathbb{H}_U^{(D\to D)}$ denotes a Uniform kernel decomposition framework in which both the trend and fluctuation components are modeled with neural-network autoregressive models. Therefore, the proposed notation system provides a mathematically rigorous, scalable, and interpretable representation of the complete kernel regression-based hybrid forecasting framework, facilitating systematic comparison and performance evaluation across all proposed forecasting architectures.

2.4. *Expanding-window one-step-ahead forecasting procedure*

The forecasting experiments are conducted using an expanding-window forecasting framework. Let t denote the forecasting origin. At each iteration, only observations available up to time t are used for kernel decomposition, model estimation, and forecast generation. A one-step-ahead forecast for time $(t + 1)$ was then produced. The newly observed value is then added to the estimation sample, and the procedure is repeated sequentially until the end of the evaluation period. Thus, no information prior to the forecasting horizon is used in the decomposition and forecasting steps, respectively, eliminating the possibility of look-ahead bias/information leakage. The empirical analysis uses daily energy commodity time series data spanning January 2016 to December 2025. The first seven years (January 2016–December 2022) are used as the initial estimation sample, while the remaining three years (January 2023–December 2025) are reserved for out-of-sample forecasting evaluation. Forecasts are generated recursively under the expanding-window framework throughout the testing period.

2.5. *Computational complexity and scalability*

Table 2 summarizes the approximate computational complexity of the forecasting models employed in this study together with their relative training requirements and interpretability.

In Table 2, N denotes the number of observations, p and q represent the autoregressive and moving-average orders, respectively, k is the number of hidden neurons in the NNAR model, and E denotes the number of training epochs. However, kernel regression decomposition adds an additional preprocessing step with a computational complexity of about $O(N^2)$ when using the usual local kernel smoothing implementation. However, this cost occurs just once at each forecasting origin in the expanding-window procedure. Forecasting models are fitted to statistically simple trend and fluctuation components, obtained after decomposition, rather than to the original highly volatile series. This separation reduces structural complexity, facilitates parameter estimation, and improves model convergence, especially for nonlinear forecasting models. On the other hand, the NNAR-based hybrid models are computationally more demanding than linear models. However, the proposed framework is still computationally feasible for daily financial and energy market datasets. The empirical study is based on some ten years of daily observations, and all hybrid models can be efficiently estimated by standard implementations in the `R` environment.

Table 2. Qualitative comparison of computational complexity and training characteristics of the forecasting models.

Model	Type	Approximate Complexity	Training Time	Interpretability
AR	Linear	$O(Np^2)$	Very Low	High
ARIMA	Linear	$O(N(p+q)^2)$	Low	High
NPAR	Nonparametric	$O(N^2)$	Moderate	Moderate
NNAR	Nonlinear	$O(NEpk)$	High	Low

2.6. *Performance evaluation metrics*

In this work, several statistical measures of accuracy and efficiency are used to examine the forecasting performance in detail. The mathematical equations for the following measurements are in Table 3. These include the Mean Absolute Error (MAE), Root Mean Square Error (RMSE), Mean Absolute Percentage Error (MAPE), Correlation Coefficient (CORR), Directional Accuracy (DA), Nash-Sutcliffe Efficiency (NSE), and Kling-Gupta Efficiency (KGE).

Table 3. Evaluation metrics.

Metric	Mathematical Expression
MAE	$\frac{1}{N}\sum_{t=1}^{N}\left\lvert X_t^{(m)}-\widehat{X}_t^{(m)}\right\rvert$
RMSE	$\sqrt{\frac{1}{N}\sum_{t=1}^{N}\left(X_t^{(m)}-\widehat{X}_t^{(m)}\right)^2}$
MAPE	$\frac{100}{N}\sum_{t=1}^{N}\left\lvert\frac{X_t^{(m)}-\widehat{X}_t^{(m)}}{X_t^{(m)}}\right\rvert$
CORR	$\frac{\sum_{t=1}^{N}\left(X_t^{(m)}-\bar{X}^{(m)}\right)\left(\widehat{X}_t^{(m)}-\bar{\widehat{X}}^{(m)}\right)}{\sqrt{\sum_{t=1}^{N}\left(X_t^{(m)}-\bar{X}^{(m)}\right)^2}\sqrt{\sum_{t=1}^{N}\left(\widehat{X}_t^{(m)}-\bar{\widehat{X}}^{(m)}\right)^2}}$
DA	$\frac{1}{N-1}\sum_{t=2}^{N}\mathbb{I}\left[\left(X_t^{(m)}-X_{t-1}^{(m)}\right)\left(\widehat{X}_t^{(m)}-\widehat{X}_{t-1}^{(m)}\right)>0\right]$
NSE	$1-\frac{\sum_{t=1}^{N}\left(X_t^{(m)}-\widehat{X}_t^{(m)}\right)^2}{\sum_{t=1}^{N}\left(X_t^{(m)}-\bar{X}^{(m)}\right)^2}$
KGE	$1-\sqrt{(r-1)^2+\left(\frac{\mu_s}{\mu_o}-1\right)^2+\left(\frac{\sigma_s}{\sigma_o}-1\right)^2}$

In addition, to further assess the statistical significance of the forecasting improvements achieved by the proposed kernel regression-based hybrid framework, the Diebold-Mariano (DM) test [64] is employed. The DM test evaluates whether the predictive performance of two competing forecasting models differs significantly. Let $e_{1,t}$ and $e_{2,t}$ denote the forecast errors generated by two competing forecasting models at time t. Based on a specified loss function $L(\cdot)$, the loss differential is defined as,

$d_t = L(e_{1,t}) - L(e_{2,t}), \qquad t = 1, 2, \ldots, T$, where T denotes the total number of out-of-sample forecasts. In this study, the squared-error loss function, $L(e_t) = e_t^2$, is adopted. The null hypothesis states that the proposed model does not outperform the benchmark, whereas the alternative hypothesis indicates that the proposed model has a lower expected forecast loss. Specifically, H_0 :; $E(d_t) \geq 0$, against the one-sided alternative, H_1 :; $E(d_t) < 0$, rejection of the null hypothesis indicates that the proposed forecasting model achieves significantly superior predictive accuracy compared with the competing model.

The DM test statistic is computed as $DM = \frac{\bar{d}}{\sqrt{\widehat{\mathrm{Var}}(\bar{d})}}$, where $\bar{d} = \frac{1}{T}\sum_{t=1}^{T} d_t$, is the sample mean of the loss differential, and $\widehat{\mathrm{Var}}(\bar{d})$ denotes a consistent estimate of its variance that accounts for possible serial correlation in the forecast loss differentials. Under the null hypothesis, the DM statistic is asymptotically standard normal, $DM \sim N(0, 1)$. In this study, the DM test is employed to compare the proposed kernel regression-based hybrid forecasting models with the best-performing direct hybrid and standalone forecasting models for each energy commodity market. Consequently, the DM test complements conventional forecasting accuracy measures by providing statistical evidence of the significance of the observed improvements in forecasting accuracy.

To conclude this section, the full system of the proposed forecasting framework is illustrated in Figure 1.

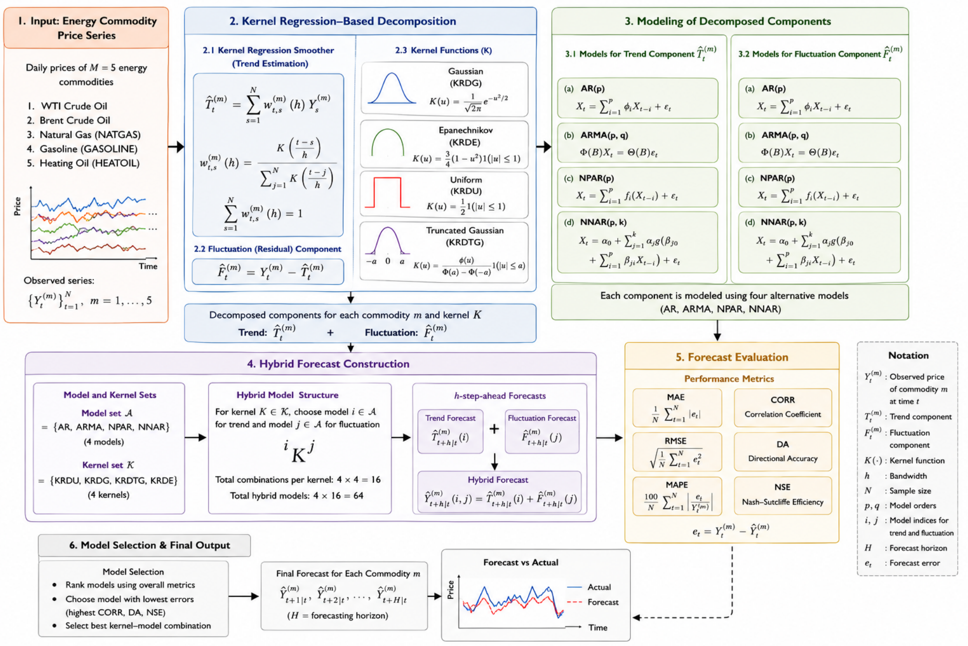

Figure 1. Complete flowchart of the proposed forecasting framework.

3. Results

In this paper, we proposed the kernel regression-based decomposition forecasting framework and applied it to five major global energy markets, namely WTI and Brent crude oil, NATGAS, GASOLINE, and HEATOIL, to obtain one-day-ahead (short-term) forecasts. Each energy price time series was carefully examined for missing values and data consistency before the empirical analysis;

no missing observations were detected. Therefore, no imputation procedures were required; similarly, no outliers were removed because extreme price movements represent genuine market behavior and are essential for evaluating forecasting models under realistic energy market conditions. Only the WTI series contained a single negative price observation (20 April 2020), reflecting the unprecedented market conditions during the COVID-19 pandemic. Because the logarithmic transformation is undefined for non-positive values, this isolated observation was removed before applying the logarithmic transformation. Since only one observation was affected, its removal had a negligible impact on the temporal continuity of the series. The expanding-window forecasting procedure was subsequently performed sequentially on the remaining chronologically ordered observations without introducing any future information. Forecasts were generated on the logarithmic scale and then back-transformed to the original price scale using the inverse exponential transformation. Forecasting accuracy measures were computed on the original price scale, and no additional bias correction was applied during back-transformation because the same transformation procedure was used consistently for all competing forecasting models. The data are daily observations over 10 years (from January 2016 to December 2025) for the world's major energy commodities, which play fundamental roles in global energy supply chains, industrial production, transportation systems, and overall economic activity, and are obtained from Yahoo Finance. A rigorous chronological train-test split was utilized across the forecasting experiment to avoid data leakage. The first seven years of data (January 2016–December 2022) were used only to perform kernel regression decomposition, bandwidth selection, model estimation, and parameter tuning; the last three years (January 2023–December 2025) were reserved only for out-of-sample forecasting evaluation. The trend and fluctuation components were estimated using only the training data. All the forecasting models were fitted to the corresponding decomposed training series. The forecasts for the testing period were made sequentially without using any future observations, which gave an unbiased and realistic evaluation of the proposed kernel regression-based hybrid forecasting framework.

The energy commodity price series is shown in Figure 2 for visual analysis. The visual analysis shows that the series is highly nonlinear and non-stationary, with persistent long-term trends, abrupt structural breaks, volatility clustering, and large price swings over time. Major market disruptions have been caused by the COVID-19 pandemic, geopolitical conflicts, global supply chain instability, and shocks to the energy markets. Specifically, WTI and Brent crude oil prices have large shocks in the long run, while NATGAS has large volatility spikes due to seasonal demand and geopolitical uncertainties in supply. Refinery activity, the need for transportation, and the way in which crude oil prices are passed through also influence the volatility of gasoline and heating oil.

Table 4 shows the descriptive statistics and statistical features of five major energy commodity price series: The original, logarithmic, and differenced logarithmic. The results suggest several common features across all energy markets. The original price series is very volatile, with large dynamic ranges and high nonlinearity, which is indicative of the inherent instability of global energy markets. WTI crude oil prices have the highest price volatility, including negative prices during the COVID-19 pandemic. Brent crude oil prices are very sensitive to geopolitical events and production policies. NATGAS displays the highest relative volatility and strong positive skewness and kurtosis, implying frequent extreme price movements and heavy-tailed behavior. Gasoline and heating oil have similar distributional characteristics. The logarithmic transformation and first differencing significantly improve stationarity, as confirmed by the ADF test, but the JB and ARCH tests indicate that nonnormality and conditional heteroscedasticity are still statistically significant. Seasonality is particularly apparent in NATGAS and GASOLINE, driven by weather, energy demand, and refinery activity. The empirical analysis strongly supports the view that energy commodity prices are best described by nonstationarity, nonlinearity, heavy tails, volatility clustering, and seasonal dynamics, which strongly justifies the use of the proposed kernel regression-based decomposition framework that separates the long-run trend from the short-run fluctuations for better forecasting. In addition, the combined application of different kernel functions with linear and non-linear forecasting models such as AR, ARIMA, NPAR, and NNAR results in a flexible and robust approach for modeling the heterogeneous behavior of WTI, Brent, NATGAS, GASOLINE, and HEATOIL markets and, thus, enhances prediction accuracy and stability across various energy segments.

Figure 2. Time series plot for all considered energy commodity markets.

The proposed framework for predictive modeling decomposes energy price time series into long-term trend (T_t) and short-run fluctuation (F_t) components. This was done using the kernel regression-based decomposition approach and four different kernel specifications: Uniform ($\mathbb{H}_U$), Gaussian ($\mathbb{H}_G$), Truncated Gaussian ($\mathbb{H}_{TG}$), and Epanechnikov ($\mathbb{H}_E$). With the trend and fluctuation components decomposed, linear and nonlinear forecasting models are fitted separately. Linear AR and ARIMA models were used for linear forecasting, while nonlinear NPAR and NNAR models were used for nonlinear forecasting. Hybridization structures may be linear-linear, nonlinear-nonlinear, or a hybrid of both. The proposed framework can therefore accommodate all three. In each kernel decomposition, sixteen hybrid forecasting structures are produced, since four forecasting models were used for the trend and fluctuation components. For each energy commodity price, sixty-four hybrid forecasting models were tested, covering all four kernel functions. The one-step-ahead predicting performance measures, which included MAPE, MAE, RMSE, CORR, DA, NSE, and KGE, are presented in Table 5 for WTI, Table 6 for Brent, Table 7 for NATGAS, Table 8 for GASOLINE, and Table 9 for HEATOIL markets.

For the WTI market, the hybrid model $\mathbb{H}_E^{(D\to D)}$, based on the Epanechnikov kernel and combining NNAR forecasting of both trend and fluctuation components, achieves the best forecasting performance (see Table 5). For this model, the lowest forecasting errors are obtained with MAPE = 0.4421, MAE = 0.3092, and RMSE = 0.4031, and it provides excellent goodness-of-fit metrics (CORR = 0.9988, NSE = 0.9973, and KGE = 0.9908). The model has strong directional forecasting ability with DA = 0.8867, demonstrating its ability to capture short-term market fluctuations. The excellent performance of the Epanechnikov kernel demonstrates that the adaptive local smoothing can eliminate high-frequency noise while preserving important structural information. The uniform kernel-based hybrids always produce the lowest forecasting accuracy, suggesting that equal-weight smoothing is less suitable for capturing sudden volatility switches and nonlinear relationships in WTI prices.

On the other hand, the uniform kernel-based hybrid $\mathbb{H}_U^{(I\to D)}$ exhibits the best forecasting performance for the Brent crude oil dataset (Table 6) with MAPE = 0.4372, MAE = 0.3198, and RMSE = 0.4339. The model has obtained high predictive efficiency indices such as CORR = 0.9987, NSE = 0.9971, and KGE = 0.9928 and good directional accuracy (DA = 0.8473). The consistent outperformance of uniform kernel-based models across various hybrid setups shows that balanced neighborhood smoothing can capture the essential temporal characteristics of Brent prices. Furthermore, hybrid models that integrate linear models for the trend element and nonlinear NNAR structures for the fluctuation component generally outperform purely linear models, indicating the presence of both stable long-term behavior and nonlinear short-term volatility patterns in Brent markets.

Table 4. All descriptive statistics and diagnostic measurements of energy commodity prices are level, logarithmic, and differenced logarithmic transformed.

Series	Type	Min	Max	Mean	Median	Mode	Q1	Q2	Q3	Variance	SD	CoefVar	Skewness	Kurtosis	ADF_Stat	JB_Stat	ARCH_Stat
WTI	Level	-37.63	123.70	63.48	63.37	67.04	51.64	63.37	74.11	300.71	17.34	0.27	0.19	3.95	-2.42	87.74	1991.39
WTI	Log	2.30	4.82	4.11	4.15	4.21	3.94	4.15	4.31	0.09	0.29	0.07	-0.93	5.55	-2.83	NA	1995.72
WTI	Diff_Log	-0.28	0.42	0.00	0.00	0.00	-0.01	0.00	0.01	0.00	0.03	56.23	1.06	35.71	-11.00	NA	437.42
BRENT	Level	19.33	127.98	67.77	67.76	74.74	55.71	67.76	79.13	311.65	17.65	0.26	0.16	3.26	-2.30	14.85	1991.91
BRENT	Log	2.96	4.85	4.18	4.22	4.31	4.02	4.22	4.37	0.08	0.28	0.07	-0.77	4.06	-2.62	298.09	2000.84
BRENT	Diff_Log	-0.28	0.21	0.00	0.00	0.00	-0.01	0.00	0.01	0.00	0.03	108.74	-0.88	18.81	-13.04	21406.17	352.87
NATGAS	Level	1.48	9.68	3.22	2.86	2.75	2.48	2.86	3.42	1.87	1.37	0.43	2.12	8.08	-2.79	3702.25	1971.87
NATGAS	Log	0.39	2.27	1.10	1.05	1.01	0.91	1.05	1.23	0.12	0.35	0.32	0.93	4.09	-2.73	394.34	1986.69
NATGAS	Diff_Log	-0.30	0.38	0.00	0.00	0.00	-0.02	0.00	0.02	0.00	0.04	168.82	0.25	8.56	-12.25	2635.01	199.05
GASOLINE	Level	0.41	4.28	1.97	1.97	1.47	1.58	1.97	2.26	0.32	0.56	0.29	0.64	4.26	-2.57	275.02	1992.67
GASOLINE	Log	-0.89	1.45	0.63	0.68	0.39	0.46	0.68	0.82	0.09	0.30	0.47	-0.64	4.84	-3.07	423.12	1991.13
GASOLINE	Diff_Log	-0.51	0.29	0.00	0.00	-0.03	-0.01	0.00	0.01	0.00	0.03	231.63	-2.10	44.56	-12.38	147584.31	222.49
HEATOIL	Level	0.61	5.14	2.15	2.09	1.24	1.65	2.09	2.47	0.48	0.69	0.32	0.77	3.82	-1.95	255.78	1977.55
HEATOIL	Log	-0.49	1.64	0.71	0.74	0.21	0.50	0.74	0.90	0.11	0.32	0.46	-0.23	3.15	-2.19	19.73	1997.15

Table 5. The out-of-sample one-step-ahead forecasting accuracy of all sixty-four hybrid models for the WTI oil prices employing the proposed forecasting framework.

S.No	Model	MAPE	MAE	RMSE	CORR	DA	NSE	KGE
1	$\mathbb{H}_{G}^{(A\to A)}$	0.4784	0.3339	0.4415	0.9983	0.8916	0.9965	0.9881
2	$\mathbb{H}_{G}^{(A\to I)}$	0.4787	0.3342	0.4418	0.9982	0.8892	0.9964	0.9879
3	$\mathbb{H}_{G}^{(A\to N)}$	0.4762	0.3321	0.4397	0.9984	0.8941	0.9966	0.9888
4	$\mathbb{H}_{G}^{(A\to D)}$	0.4748	0.3312	0.4386	0.9985	0.8966	0.9968	0.9893
5	$\mathbb{H}_{G}^{(I\to A)}$	0.4757	0.3327	0.4442	0.9983	0.8941	0.9965	0.9885
6	$\mathbb{H}_{G}^{(I\to I)}$	0.4761	0.3331	0.4446	0.9982	0.8916	0.9964	0.9882
7	$\mathbb{H}_{G}^{(I\to N)}$	0.4734	0.3310	0.4418	0.9984	0.8966	0.9967	0.9891
8	$\mathbb{H}_{G}^{(I\to D)}$	0.4719	0.3299	0.4407	0.9985	0.8990	0.9969	0.9896
9	$\mathbb{H}_{G}^{(N\to A)}$	0.4870	0.3392	0.4456	0.9983	0.8547	0.9965	0.9879
10	$\mathbb{H}_{G}^{(N\to I)}$	0.4875	0.3397	0.4462	0.9982	0.8522	0.9964	0.9876
11	$\mathbb{H}_{G}^{(N\to N)}$	0.4841	0.3371	0.4438	0.9984	0.8596	0.9966	0.9887
12	$\mathbb{H}_{G}^{(N\to D)}$	0.4826	0.3360	0.4424	0.9985	0.8621	0.9968	0.9892
13	$\mathbb{H}_{G}^{(D\to A)}$	0.4595	0.3208	0.4237	0.9984	0.8596	0.9968	0.9895
14	$\mathbb{H}_{G}^{(D\to I)}$	0.4599	0.3212	0.4241	0.9983	0.8571	0.9967	0.9892
15	$\mathbb{H}_{G}^{(D\to N)}$	0.4568	0.3189	0.4214	0.9985	0.8645	0.9969	0.9902
16	$\mathbb{H}_{G}^{(D\to D)}$	0.4552	0.3177	0.4201	0.9986	0.8670	0.9970	0.9908
17	$\mathbb{H}_{E}^{(A\to A)}$	0.5325	0.3720	0.4977	0.9979	0.8719	0.9956	0.9876
18	$\mathbb{H}_{E}^{(A\to I)}$	0.5330	0.3725	0.4982	0.9978	0.8695	0.9955	0.9873
19	$\mathbb{H}_{E}^{(A\to N)}$	0.5284	0.3691	0.4926	0.9980	0.8768	0.9958	0.9884
20	$\mathbb{H}_{E}^{(A\to D)}$	0.5259	0.3673	0.4898	0.9981	0.8793	0.9960	0.9890
21	$\mathbb{H}_{E}^{(I\to A)}$	0.5217	0.3644	0.4846	0.9980	0.8818	0.9958	0.9880
22	$\mathbb{H}_{E}^{(I\to I)}$	0.5222	0.3649	0.4850	0.9979	0.8793	0.9957	0.9877
23	$\mathbb{H}_{E}^{(I\to N)}$	0.5183	0.3620	0.4801	0.9981	0.8842	0.9959	0.9888
24	$\mathbb{H}_{E}^{(I\to D)}$	0.5157	0.3601	0.4774	0.9982	0.8867	0.9961	0.9893
25	$\mathbb{H}_{E}^{(N\to A)}$	0.4571	0.3202	0.4164	0.9985	0.8842	0.9969	0.9876
26	$\mathbb{H}_{E}^{(N\to I)}$	0.4575	0.3206	0.4169	0.9984	0.8818	0.9968	0.9873
27	$\mathbb{H}_{E}^{(N\to N)}$	0.4532	0.3175	0.4128	0.9986	0.8892	0.9970	0.9885
28	$\mathbb{H}_{E}^{(N\to D)}$	0.4506	0.3156	0.4103	0.9987	0.8916	0.9972	0.9892
29	$\mathbb{H}_{E}^{(D\to A)}$	0.4481	0.3135	0.4090	0.9986	0.8793	0.9970	0.9894
30	$\mathbb{H}_{E}^{(D\to I)}$	0.4486	0.3139	0.4095	0.9985	0.8768	0.9969	0.9891
31	$\mathbb{H}_{E}^{(D\to N)}$	0.4447	0.3110	0.4057	0.9987	0.8842	0.9971	0.9901
32	$\mathbb{H}_{E}^{(D\to D)}$	0.4421	0.3092	0.4031	0.9988	0.8867	0.9973	0.9908
33	$\mathbb{H}_{U}^{(A\to A)}$	0.8095	0.5653	0.7598	0.9949	0.7414	0.9898	0.9913
34	$\mathbb{H}_{U}^{(A\to I)}$	0.8101	0.5659	0.7605	0.9948	0.7389	0.9897	0.9910
35	$\mathbb{H}_{U}^{(A\to N)}$	0.8048	0.5618	0.7552	0.9950	0.7463	0.9899	0.9918
36	$\mathbb{H}_{U}^{(A\to D)}$	0.8019	0.5597	0.7526	0.9951	0.7488	0.9901	0.9922
37	$\mathbb{H}_{U}^{(I\to A)}$	0.8095	0.5653	0.7598	0.9949	0.7414	0.9898	0.9913
38	$\mathbb{H}_{U}^{(I\to I)}$	0.8100	0.5658	0.7604	0.9948	0.7389	0.9897	0.9910
39	$\mathbb{H}_{U}^{(I\to N)}$	0.8045	0.5615	0.7549	0.9950	0.7488	0.9899	0.9918
40	$\mathbb{H}_{U}^{(I\to D)}$	0.8016	0.5593	0.7521	0.9951	0.7512	0.9901	0.9923
41	$\mathbb{H}_{U}^{(N\to A)}$	1.1385	0.7940	1.0779	0.9897	0.7241	0.9794	0.9817
42	$\mathbb{H}_{U}^{(N\to I)}$	1.1392	0.7947	1.0788	0.9896	0.7217	0.9793	0.9814
43	$\mathbb{H}_{U}^{(N\to N)}$	1.1326	0.7898	1.0712	0.9899	0.7291	0.9797	0.9823
44	$\mathbb{H}_{U}^{(N\to D)}$	1.1284	0.7869	1.0675	0.9900	0.7315	0.9799	0.9828
45	$\mathbb{H}_{U}^{(D\to A)}$	1.1396	0.7946	1.0813	0.9896	0.7266	0.9792	0.9881
46	$\mathbb{H}_{U}^{(D\to I)}$	1.1403	0.7952	1.0821	0.9895	0.7241	0.9791	0.9878
47	$\mathbb{H}_{U}^{(D\to N)}$	1.1344	0.7908	1.0753	0.9898	0.7315	0.9795	0.9887
48	$\mathbb{H}_{U}^{(D\to D)}$	1.1305	0.7879	1.0714	0.9899	0.7340	0.9797	0.9892
49	$\mathbb{H}_{TG}^{(A\to A)}$	0.4760	0.3324	0.4388	0.9983	0.8719	0.9966	0.9896
50	$\mathbb{H}_{TG}^{(A\to I)}$	0.4765	0.3329	0.4393	0.9982	0.8695	0.9965	0.9893
51	$\mathbb{H}_{TG}^{(A\to N)}$	0.4724	0.3299	0.4352	0.9984	0.8768	0.9967	0.9903
52	$\mathbb{H}_{TG}^{(A\to D)}$	0.4698	0.3280	0.4326	0.9985	0.8793	0.9969	0.9910
53	$\mathbb{H}_{TG}^{(I\to A)}$	0.4854	0.3396	0.4534	0.9982	0.8842	0.9964	0.9891
54	$\mathbb{H}_{TG}^{(I\to I)}$	0.4859	0.3400	0.4539	0.9981	0.8818	0.9963	0.9888
55	$\mathbb{H}_{TG}^{(I\to N)}$	0.4816	0.3369	0.4487	0.9983	0.8892	0.9965	0.9898
56	$\mathbb{H}_{TG}^{(I\to D)}$	0.4789	0.3350	0.4461	0.9984	0.8916	0.9967	0.9904
57	$\mathbb{H}_{TG}^{(N\to A)}$	0.5493	0.3833	0.5101	0.9977	0.8596	0.9954	0.9871
58	$\mathbb{H}_{TG}^{(N\to I)}$	0.5499	0.3839	0.5108	0.9976	0.8571	0.9953	0.9868
59	$\mathbb{H}_{TG}^{(N\to N)}$	0.5436	0.3792	0.5034	0.9978	0.8645	0.9956	0.9879
60	$\mathbb{H}_{TG}^{(N\to D)}$	0.5398	0.3764	0.4997	0.9979	0.8670	0.9958	0.9885
61	$\mathbb{H}_{TG}^{(D\to A)}$	0.5409	0.3775	0.5053	0.9978	0.8547	0.9955	0.9868
62	$\mathbb{H}_{TG}^{(D\to I)}$	0.5415	0.3780	0.5059	0.9977	0.8522	0.9954	0.9865
63	$\mathbb{H}_{TG}^{(D\to N)}$	0.5352	0.3734	0.4986	0.9979	0.8596	0.9957	0.9876
64	$\mathbb{H}_{TG}^{(D\to D)}$	0.5314	0.3707	0.4949	0.9980	0.8621	0.9959	0.9882

Table 6. The out-of-sample one-step-ahead forecasting accuracy of all sixty-four hybrid models for the Brent oil prices employing the proposed forecasting framework.

S.No	Model	MAPE	MAE	RMSE	CORR	DA	NSE	KGE
1	$\mathbb{H}_{G}^{(A\to A)}$	1.3872	1.0185	1.3974	0.9838	0.4975	0.9677	0.9838
2	$\mathbb{H}_{G}^{(A\to I)}$	1.3874	1.0187	1.3978	0.9838	0.4951	0.9676	0.9837
3	$\mathbb{H}_{G}^{(A\to N)}$	1.3868	1.0181	1.3969	0.9839	0.5000	0.9678	0.9840
4	$\mathbb{H}_{G}^{(A\to D)}$	1.3861	1.0176	1.3958	0.9840	0.5025	0.9680	0.9843
5	$\mathbb{H}_{G}^{(I\to A)}$	1.3873	1.0186	1.3975	0.9838	0.4975	0.9677	0.9838
6	$\mathbb{H}_{G}^{(I\to I)}$	1.3875	1.0188	1.3979	0.9838	0.4951	0.9676	0.9837
7	$\mathbb{H}_{G}^{(I\to N)}$	1.3869	1.0182	1.3970	0.9839	0.5000	0.9678	0.9840
8	$\mathbb{H}_{G}^{(I\to D)}$	1.3862	1.0177	1.3959	0.9840	0.5025	0.9680	0.9843
9	$\mathbb{H}_{G}^{(N\to A)}$	1.3927	1.0225	1.3982	0.9838	0.4951	0.9677	0.9829
10	$\mathbb{H}_{G}^{(N\to I)}$	1.3929	1.0227	1.3985	0.9838	0.4926	0.9676	0.9828
11	$\mathbb{H}_{G}^{(N\to N)}$	1.3921	1.0219	1.3976	0.9839	0.4975	0.9678	0.9831
12	$\mathbb{H}_{G}^{(N\to D)}$	1.3915	1.0214	1.3968	0.9840	0.5000	0.9679	0.9834
13	$\mathbb{H}_{G}^{(D\to A)}$	1.3911	1.0209	1.4057	0.9838	0.4951	0.9672	0.9835
14	$\mathbb{H}_{G}^{(D\to I)}$	1.3913	1.0211	1.4061	0.9838	0.4926	0.9671	0.9834
15	$\mathbb{H}_{G}^{(D\to N)}$	1.3906	1.0204	1.4048	0.9839	0.4975	0.9673	0.9837
16	$\mathbb{H}_{G}^{(D\to D)}$	1.3899	1.0198	1.4039	0.9840	0.5000	0.9675	0.9840
17	$\mathbb{H}_{E}^{(A\to A)}$	1.1101	0.8141	1.1134	0.9897	0.6355	0.9796	0.9865
18	$\mathbb{H}_{E}^{(A\to I)}$	1.1103	0.8143	1.1138	0.9897	0.6330	0.9795	0.9864
19	$\mathbb{H}_{E}^{(A\to N)}$	1.1057	0.8107	1.1084	0.9898	0.6404	0.9797	0.9867
20	$\mathbb{H}_{E}^{(A\to D)}$	1.1049	0.8101	1.1076	0.9899	0.6429	0.9799	0.9870
21	$\mathbb{H}_{E}^{(I\to A)}$	0.9698	0.7121	0.9657	0.9923	0.6453	0.9847	0.9909
22	$\mathbb{H}_{E}^{(I\to I)}$	0.9701	0.7124	0.9660	0.9923	0.6429	0.9846	0.9908
23	$\mathbb{H}_{E}^{(I\to N)}$	0.9658	0.7090	0.9605	0.9924	0.6478	0.9848	0.9911
24	$\mathbb{H}_{E}^{(I\to D)}$	0.9651	0.7085	0.9598	0.9925	0.6502	0.9850	0.9914
25	$\mathbb{H}_{E}^{(N\to A)}$	1.1092	0.8131	1.1141	0.9897	0.6355	0.9795	0.9860
26	$\mathbb{H}_{E}^{(N\to I)}$	1.1094	0.8133	1.1144	0.9897	0.6330	0.9794	0.9859
27	$\mathbb{H}_{E}^{(N\to N)}$	1.1053	0.8101	1.1094	0.9898	0.6404	0.9796	0.9862
28	$\mathbb{H}_{E}^{(N\to D)}$	1.1046	0.8095	1.1086	0.9899	0.6429	0.9798	0.9865
29	$\mathbb{H}_{E}^{(D\to A)}$	1.1122	0.8151	1.1195	0.9897	0.6330	0.9793	0.9895
30	$\mathbb{H}_{E}^{(D\to I)}$	1.1124	0.8153	1.1198	0.9897	0.6305	0.9792	0.9894
31	$\mathbb{H}_{E}^{(D\to N)}$	1.1083	0.8121	1.1149	0.9898	0.6355	0.9795	0.9897
32	$\mathbb{H}_{E}^{(D\to D)}$	1.1076	0.8115	1.1141	0.9899	0.6379	0.9797	0.9900
33	$\mathbb{H}_{U}^{(A\to A)}$	0.4532	0.3321	0.4506	0.9984	0.8325	0.9967	0.9932
34	$\mathbb{H}_{U}^{(A\to I)}$	0.4534	0.3323	0.4510	0.9984	0.8300	0.9966	0.9931
35	$\mathbb{H}_{U}^{(A\to N)}$	0.4461	0.3264	0.4448	0.9985	0.8399	0.9968	0.9934
36	$\mathbb{H}_{U}^{(A\to D)}$	0.4453	0.3258	0.4439	0.9986	0.8424	0.9970	0.9937
37	$\mathbb{H}_{U}^{(I\to A)}$	0.4441	0.3253	0.4403	0.9985	0.8399	0.9969	0.9923
38	$\mathbb{H}_{U}^{(I\to I)}$	0.4443	0.3255	0.4407	0.9985	0.8374	0.9968	0.9922
39	$\mathbb{H}_{U}^{(I\to N)}$	0.4380	0.3204	0.4347	0.9986	0.8448	0.9970	0.9925
40	$\mathbb{H}_{U}^{(I\to D)}$	0.4372	0.3198	0.4339	0.9987	0.8473	0.9971	0.9928
41	$\mathbb{H}_{U}^{(N\to A)}$	0.4848	0.3547	0.4819	0.9982	0.8424	0.9962	0.9919
42	$\mathbb{H}_{U}^{(N\to I)}$	0.4850	0.3549	0.4822	0.9982	0.8399	0.9961	0.9918
43	$\mathbb{H}_{U}^{(N\to N)}$	0.4785	0.3495	0.4743	0.9983	0.8448	0.9963	0.9920
44	$\mathbb{H}_{U}^{(N\to D)}$	0.4777	0.3489	0.4735	0.9984	0.8473	0.9965	0.9923
45	$\mathbb{H}_{U}^{(D\to A)}$	0.4829	0.3534	0.4748	0.9982	0.8424	0.9963	0.9933
46	$\mathbb{H}_{U}^{(D\to I)}$	0.4831	0.3536	0.4751	0.9982	0.8399	0.9962	0.9932
47	$\mathbb{H}_{U}^{(D\to N)}$	0.4760	0.3478	0.4674	0.9983	0.8448	0.9964	0.9935
48	$\mathbb{H}_{U}^{(D\to D)}$	0.4752	0.3472	0.4666	0.9984	0.8473	0.9966	0.9938
49	$\mathbb{H}_{TG}^{(A\to A)}$	1.1833	0.8683	1.1893	0.9883	0.5837	0.9767	0.9863
50	$\mathbb{H}_{TG}^{(A\to I)}$	1.1835	0.8685	1.1896	0.9883	0.5813	0.9766	0.9862
51	$\mathbb{H}_{TG}^{(A\to N)}$	1.1802	0.8659	1.1854	0.9884	0.5862	0.9768	0.9865
52	$\mathbb{H}_{TG}^{(A\to D)}$	1.1795	0.8653	1.1846	0.9885	0.5887	0.9770	0.9868
53	$\mathbb{H}_{TG}^{(I\to A)}$	1.1106	0.8156	1.1131	0.9898	0.5911	0.9796	0.9890
54	$\mathbb{H}_{TG}^{(I\to I)}$	1.1108	0.8158	1.1134	0.9898	0.5887	0.9795	0.9889
55	$\mathbb{H}_{TG}^{(I\to N)}$	1.1082	0.8137	1.1094	0.9899	0.5936	0.9797	0.9892
56	$\mathbb{H}_{TG}^{(I\to D)}$	1.1075	0.8132	1.1086	0.9900	0.5961	0.9799	0.9895
57	$\mathbb{H}_{TG}^{(N\to A)}$	1.1837	0.8681	1.1902	0.9883	0.5837	0.9766	0.9858
58	$\mathbb{H}_{TG}^{(N\to I)}$	1.1839	0.8683	1.1905	0.9883	0.5813	0.9765	0.9857
59	$\mathbb{H}_{TG}^{(N\to N)}$	1.1807	0.8657	1.1865	0.9884	0.5862	0.9767	0.9859
60	$\mathbb{H}_{TG}^{(N\to D)}$	1.1800	0.8651	1.1857	0.9885	0.5887	0.9769	0.9862
61	$\mathbb{H}_{TG}^{(D\to A)}$	1.1798	0.8649	1.1922	0.9883	0.5837	0.9765	0.9883
62	$\mathbb{H}_{TG}^{(D\to I)}$	1.1800	0.8651	1.1925	0.9883	0.5813	0.9764	0.9882
63	$\mathbb{H}_{TG}^{(D\to N)}$	1.1771	0.8628	1.1887	0.9884	0.5862	0.9767	0.9884
64	$\mathbb{H}_{TG}^{(D\to D)}$	1.1764	0.8622	1.1879	0.9885	0.5887	0.9768	0.9887

In the NATGAS market case, the results are reported in Table 7. In this market, the best forecasting accuracy ($MAPE = 0.5501$, $MAE = 0.0119$ and $RMSE = 0.0164$) is for the model $\mathbb{H}_E^{(I\to N)}$ using the Epanechnikov kernel. The model shows good goodness-of-fit statistics (CORR = 0.9979, NSE = 0.9958, and KGE = 0.9939) and significant directional forecasting ability (DA = 0.8300). The results show that adaptive weighted smoothing is highly effective at modeling the volatile, irregular nature of natural gas prices. The Epanechnikov kernel decomposition is superior to the Gaussian and Truncated Gaussian kernel decompositions at capturing localized nonlinear fluctuations and abrupt volatility shifts, hallmarks of natural gas markets.

The same is valid for the GASOLINE market (Table 8), where the Uniform kernel-based hybrid $\mathbb{H}_U^{(I\to N)}$ provides the most accurate predictions with MAPE = 0.4342, MAE = 0.0102, and RMSE = 0.0134. Moreover, the model has excellent efficiency values with CORR = 0.9978, NSE = 0.9955, and KGE = 0.9887. The good performance of the Uniform kernel suggests that the gasoline price fluctuations exhibit relatively stable local dependence structures that are enhanced by balanced smoothing in decomposition. However, models that use Gaussian and Truncated Gaussian kernels tend to produce larger forecast errors, suggesting a reduced ability to capture local market anomalies.

For the HEATOIL market (Table 9), the hybrid model $\mathbb{H}_E^{(I\to D)}$ with the Epanechnikov kernel shows better prediction performance with the minimum forecasting errors in terms of MAPE = 0.0849, MAE = 0.0009, and RMSE = 0.0012. The model shows very good goodness of fit measures (CORR = 0.9994, NSE = 0.9987, and KGE = 0.9958), confirming its strong predictive ability. The results show that the Epanechnikov kernel can capture persistent trend structures and short-term nonlinear volatility patterns in heating oil prices. For all commodity datasets, hybrid structures with nonlinear forecasting for the fluctuation part performed consistently better than purely linear ones. In addition, the kernel decomposition methods show different forecasting performance in energy commodity markets. The Epanechnikov and Uniform kernels outperform the Gaussian and Truncated Gaussian kernels, implying that adaptive local smoothing and equal weighting of neighborhoods are better able to capture non-linear market dynamics. On the other hand, the Gaussian and Truncated Gaussian kernels tend to oversmooth the series, reducing their ability to react to sudden market changes. The results show the effectiveness and robustness of the proposed kernel regression-based hybrid framework, which separates long-run trends and short-run fluctuations, enabling more accurate forecasts of nonlinear, nonstationary, and highly volatile energy commodity prices.

The proposed forecasting framework is contrasted with direct hybrid (Table 10) and standalone (Table 11) forecasting models to further evaluate the contribution of decomposition. As shown in both tables, the decomposition-based approach consistently outperforms the direct hybrids across all energy commodities. This makes it possible to learn heterogeneous temporal dynamics more effectively, which improves directional forecasting accuracy and reduces forecasting errors. The biggest improvements are in HEATOIL and NATGAS, with forecasting errors reduced by over 94% in both. On the other hand, in single forecasting models, AR, ARIMA, NPAR, and NNAR alone fail to adequately capture the nonlinear, nonstationary, and multi-scale features of energy commodity prices.

Table 7. The out-of-sample one-step-ahead forecasting accuracy of all sixty-four hybrid models for the NATGAS prices employing the proposed forecasting framework.

S.No	Model	MAPE	MAE	RMSE	CORR	DA	NSE	KGE
1	$\mathbb{H}_G^{(A\to A)}$	1.0095	0.0218	0.0310	0.9923	0.6355	0.9846	0.9904
2	$\mathbb{H}_G^{(A\to I)}$	1.0092	0.0218	0.0309	0.9923	0.6379	0.9847	0.9905
3	$\mathbb{H}_G^{(A\to N)}$	1.0031	0.0217	0.0308	0.9924	0.6404	0.9848	0.9906
4	$\mathbb{H}_G^{(A\to D)}$	1.0060	0.0217	0.0309	0.9924	0.6429	0.9848	0.9907
5	$\mathbb{H}_G^{(I\to A)}$	1.0115	0.0219	0.0310	0.9923	0.6355	0.9846	0.9903
6	$\mathbb{H}_G^{(I\to I)}$	1.0111	0.0218	0.0310	0.9923	0.6379	0.9847	0.9904
7	$\mathbb{H}_G^{(I\to N)}$	1.0050	0.0217	0.0308	0.9924	0.6429	0.9848	0.9905
8	$\mathbb{H}_G^{(I\to D)}$	1.0079	0.0218	0.0309	0.9924	0.6453	0.9848	0.9906
9	$\mathbb{H}_G^{(N\to A)}$	1.0141	0.0219	0.0311	0.9922	0.6453	0.9845	0.9886
10	$\mathbb{H}_G^{(N\to I)}$	1.0137	0.0219	0.0310	0.9922	0.6478	0.9846	0.9887
11	$\mathbb{H}_G^{(N\to N)}$	1.0076	0.0218	0.0309	0.9923	0.6502	0.9847	0.9888
12	$\mathbb{H}_G^{(N\to D)}$	1.0104	0.0218	0.0310	0.9923	0.6527	0.9847	0.9889
13	$\mathbb{H}_G^{(D\to A)}$	1.0150	0.0219	0.0311	0.9922	0.6453	0.9845	0.9887
14	$\mathbb{H}_G^{(D\to I)}$	1.0145	0.0219	0.0310	0.9922	0.6478	0.9846	0.9888
15	$\mathbb{H}_G^{(D\to N)}$	1.0092	0.0218	0.0309	0.9923	0.6502	0.9847	0.9889
16	$\mathbb{H}_G^{(D\to D)}$	1.0120	0.0218	0.0310	0.9923	0.6527	0.9847	0.9890
17	$\mathbb{H}_E^{(A\to A)}$	0.6682	0.0145	0.0203	0.9967	0.7685	0.9934	0.9918
18	$\mathbb{H}_E^{(A\to I)}$	0.6660	0.0144	0.0202	0.9967	0.7709	0.9935	0.9919
19	$\mathbb{H}_E^{(A\to N)}$	0.6593	0.0142	0.0201	0.9968	0.7734	0.9936	0.9920
20	$\mathbb{H}_E^{(A\to D)}$	0.6635	0.0143	0.0202	0.9968	0.7759	0.9936	0.9921
21	$\mathbb{H}_E^{(I\to A)}$	0.5591	0.0121	0.0167	0.9978	0.8251	0.9956	0.9937
22	$\mathbb{H}_E^{(I\to I)}$	0.5568	0.0120	0.0166	0.9978	0.8276	0.9957	0.9938
23	$\mathbb{H}_E^{(I\to N)}$	0.5501	0.0119	0.0164	0.9979	0.8300	0.9958	0.9939
24	$\mathbb{H}_E^{(I\to D)}$	0.5542	0.0120	0.0165	0.9979	0.8325	0.9958	0.9940
25	$\mathbb{H}_E^{(N\to A)}$	0.7940	0.0172	0.0243	0.9953	0.7488	0.9906	0.9931
26	$\mathbb{H}_E^{(N\to I)}$	0.7915	0.0171	0.0242	0.9954	0.7512	0.9907	0.9932
27	$\mathbb{H}_E^{(N\to N)}$	0.7846	0.0170	0.0241	0.9954	0.7562	0.9908	0.9933
28	$\mathbb{H}_E^{(N\to D)}$	0.7881	0.0170	0.0242	0.9954	0.7586	0.9908	0.9934
29	$\mathbb{H}_E^{(D\to A)}$	0.7950	0.0172	0.0243	0.9953	0.7488	0.9906	0.9926
30	$\mathbb{H}_E^{(D\to I)}$	0.7923	0.0171	0.0242	0.9953	0.7512	0.9907	0.9927
31	$\mathbb{H}_E^{(D\to N)}$	0.7861	0.0170	0.0241	0.9954	0.7562	0.9908	0.9928
32	$\mathbb{H}_E^{(D\to D)}$	0.7896	0.0170	0.0242	0.9954	0.7586	0.9908	0.9929
33	$\mathbb{H}_U^{(A\to A)}$	0.6927	0.0149	0.0206	0.9966	0.7906	0.9932	0.9934
34	$\mathbb{H}_U^{(A\to I)}$	0.6910	0.0149	0.0205	0.9966	0.7931	0.9933	0.9935
35	$\mathbb{H}_U^{(A\to N)}$	0.6891	0.0148	0.0203	0.9967	0.7956	0.9934	0.9936
36	$\mathbb{H}_U^{(A\to D)}$	0.6875	0.0148	0.0202	0.9967	0.7980	0.9935	0.9937
37	$\mathbb{H}_U^{(I\to A)}$	0.6846	0.0148	0.0202	0.9968	0.7759	0.9935	0.9925
38	$\mathbb{H}_U^{(I\to I)}$	0.6830	0.0147	0.0201	0.9968	0.7783	0.9936	0.9926
39	$\mathbb{H}_U^{(I\to N)}$	0.6814	0.0147	0.0200	0.9969	0.7808	0.9937	0.9927
40	$\mathbb{H}_U^{(I\to D)}$	0.6802	0.0146	0.0199	0.9969	0.7833	0.9937	0.9928
41	$\mathbb{H}_U^{(N\to A)}$	0.7150	0.0154	0.0215	0.9963	0.7808	0.9926	0.9934
42	$\mathbb{H}_U^{(N\to I)}$	0.7138	0.0153	0.0214	0.9964	0.7833	0.9927	0.9935
43	$\mathbb{H}_U^{(N\to N)}$	0.7121	0.0153	0.0213	0.9964	0.7857	0.9928	0.9936
44	$\mathbb{H}_U^{(N\to D)}$	0.7109	0.0152	0.0212	0.9965	0.7882	0.9928	0.9937
45	$\mathbb{H}_U^{(D\to A)}$	0.7157	0.0154	0.0215	0.9963	0.7783	0.9926	0.9927
46	$\mathbb{H}_U^{(D\to I)}$	0.7146	0.0153	0.0214	0.9964	0.7808	0.9927	0.9928
47	$\mathbb{H}_U^{(D\to N)}$	0.7130	0.0153	0.0213	0.9964	0.7833	0.9928	0.9929
48	$\mathbb{H}_U^{(D\to D)}$	0.7118	0.0152	0.0212	0.9965	0.7857	0.9928	0.9930
49	$\mathbb{H}_{TG}^{(A\to A)}$	1.2729	0.0275	0.0389	0.9879	0.5837	0.9759	0.9848
50	$\mathbb{H}_{TG}^{(A\to I)}$	1.2711	0.0274	0.0388	0.9880	0.5862	0.9760	0.9849
51	$\mathbb{H}_{TG}^{(A\to N)}$	1.2697	0.0273	0.0387	0.9880	0.5887	0.9761	0.9850
52	$\mathbb{H}_{TG}^{(A\to D)}$	1.2702	0.0274	0.0388	0.9880	0.5911	0.9761	0.9851
53	$\mathbb{H}_{TG}^{(I\to A)}$	1.1736	0.0254	0.0363	0.9895	0.6034	0.9790	0.9880
54	$\mathbb{H}_{TG}^{(I\to I)}$	1.1712	0.0253	0.0362	0.9896	0.6059	0.9791	0.9881
55	$\mathbb{H}_{TG}^{(I\to N)}$	1.1691	0.0252	0.0361	0.9896	0.6084	0.9792	0.9882
56	$\mathbb{H}_{TG}^{(I\to D)}$	1.1698	0.0252	0.0361	0.9896	0.6108	0.9792	0.9883
57	$\mathbb{H}_{TG}^{(N\to A)}$	1.2743	0.0275	0.0388	0.9879	0.5837	0.9759	0.9834
58	$\mathbb{H}_{TG}^{(N\to I)}$	1.2724	0.0274	0.0387	0.9880	0.5862	0.9760	0.9835
59	$\mathbb{H}_{TG}^{(N\to N)}$	1.2710	0.0273	0.0386	0.9880	0.5887	0.9761	0.9836
60	$\mathbb{H}_{TG}^{(N\to D)}$	1.2715	0.0273	0.0387	0.9880	0.5911	0.9761	0.9837
61	$\mathbb{H}_{TG}^{(D\to A)}$	1.2683	0.0274	0.0389	0.9879	0.5837	0.9758	0.9875
62	$\mathbb{H}_{TG}^{(D\to I)}$	1.2666	0.0273	0.0388	0.9880	0.5862	0.9759	0.9876
63	$\mathbb{H}_{TG}^{(D\to N)}$	1.2650	0.0272	0.0387	0.9880	0.5887	0.9760	0.9877
64	$\mathbb{H}_{TG}^{(D\to D)}$	1.2656	0.0272	0.0387	0.9880	0.5911	0.9760	0.9878

Table 8. The out-of-sample one-step-ahead forecasting accuracy of all sixty-four hybrid models for the GASOLINE prices employing the proposed forecasting framework.

S.No	Model	MAPE	MAE	RMSE	CORR	DA	NSE	KGE
1	$\mathbb{H}_{G}^{(A\to A)}$	1.2661	0.0273	0.0389	0.9879	0.5862	0.9758	0.9875
2	$\mathbb{H}_{G}^{(A\to I)}$	1.2680	0.0274	0.0390	0.9878	0.5850	0.9757	0.9874
3	$\mathbb{H}_{G}^{(A\to N)}$	1.2690	0.0275	0.0391	0.9877	0.5840	0.9756	0.9873
4	$\mathbb{H}_{G}^{(A\to D)}$	1.2700	0.0275	0.0392	0.9876	0.5830	0.9755	0.9872
5	$\mathbb{H}_{G}^{(I\to A)}$	1.5206	0.0361	0.0479	0.9704	0.5296	0.9410	0.9704
6	$\mathbb{H}_{G}^{(I\to I)}$	1.5215	0.0362	0.0480	0.9703	0.5288	0.9409	0.9703
7	$\mathbb{H}_{G}^{(I\to N)}$	1.5225	0.0363	0.0481	0.9702	0.5279	0.9408	0.9702
8	$\mathbb{H}_{G}^{(I\to D)}$	1.5235	0.0364	0.0482	0.9701	0.5270	0.9407	0.9701
9	$\mathbb{H}_{G}^{(N\to A)}$	1.5267	0.0362	0.0481	0.9701	0.5246	0.9405	0.9690
10	$\mathbb{H}_{G}^{(N\to I)}$	1.5276	0.0363	0.0482	0.9700	0.5238	0.9404	0.9689
11	$\mathbb{H}_{G}^{(N\to N)}$	1.5285	0.0364	0.0483	0.9699	0.5229	0.9403	0.9688
12	$\mathbb{H}_{G}^{(N\to D)}$	1.5294	0.0365	0.0484	0.9698	0.5220	0.9402	0.9687
13	$\mathbb{H}_{G}^{(D\to A)}$	1.5383	0.0365	0.0482	0.9700	0.5296	0.9402	0.9697
14	$\mathbb{H}_{G}^{(D\to I)}$	1.5391	0.0366	0.0483	0.9699	0.5288	0.9401	0.9696
15	$\mathbb{H}_{G}^{(D\to N)}$	1.5400	0.0367	0.0484	0.9698	0.5279	0.9400	0.9695
16	$\mathbb{H}_{G}^{(D\to D)}$	1.5408	0.0368	0.0485	0.9697	0.5270	0.9399	0.9694
17	$\mathbb{H}_{E}^{(A\to A)}$	1.5319	0.0364	0.0480	0.9703	0.5320	0.9406	0.9700
18	$\mathbb{H}_{E}^{(A\to I)}$	1.4762	0.0351	0.0465	0.9721	0.5345	0.9443	0.9720
19	$\mathbb{H}_{E}^{(A\to N)}$	1.4728	0.0350	0.0463	0.9723	0.5394	0.9447	0.9724
20	$\mathbb{H}_{E}^{(A\to D)}$	1.4746	0.0350	0.0464	0.9722	0.5370	0.9445	0.9722
21	$\mathbb{H}_{E}^{(I\to A)}$	1.4734	0.0350	0.0467	0.9718	0.5296	0.9439	0.9708
22	$\mathbb{H}_{E}^{(I\to I)}$	1.4734	0.0350	0.0467	0.9718	0.5296	0.9439	0.9708
23	$\mathbb{H}_{E}^{(I\to N)}$	1.4698	0.0349	0.0465	0.9720	0.5345	0.9443	0.9712
24	$\mathbb{H}_{E}^{(I\to D)}$	1.4715	0.0349	0.0466	0.9719	0.5320	0.9441	0.9710
25	$\mathbb{H}_{E}^{(N\to A)}$	1.4916	0.0354	0.0468	0.9717	0.5320	0.9436	0.9713
26	$\mathbb{H}_{E}^{(N\to I)}$	1.4916	0.0354	0.0468	0.9717	0.5320	0.9436	0.9713
27	$\mathbb{H}_{E}^{(N\to N)}$	1.4879	0.0353	0.0466	0.9719	0.5369	0.9440	0.9717
28	$\mathbb{H}_{E}^{(N\to D)}$	1.4898	0.0353	0.0467	0.9718	0.5345	0.9438	0.9715
29	$\mathbb{H}_{E}^{(D\to A)}$	1.4875	0.0353	0.0467	0.9720	0.5296	0.9439	0.9716
30	$\mathbb{H}_{E}^{(D\to I)}$	1.4875	0.0353	0.0467	0.9720	0.5296	0.9439	0.9716
31	$\mathbb{H}_{E}^{(D\to N)}$	1.4838	0.0352	0.0465	0.9722	0.5345	0.9443	0.9720
32	$\mathbb{H}_{E}^{(D\to D)}$	1.4857	0.0352	0.0466	0.9721	0.5320	0.9441	0.9718
33	$\mathbb{H}_{U}^{(A\to A)}$	0.4849	0.0115	0.0150	0.9971	0.8621	0.9942	0.9876
34	$\mathbb{H}_{U}^{(A\to I)}$	0.4849	0.0115	0.0150	0.9971	0.8621	0.9942	0.9876
35	$\mathbb{H}_{U}^{(A\to N)}$	0.4795	0.0113	0.0147	0.9973	0.8695	0.9947	0.9881
36	$\mathbb{H}_{U}^{(A\to D)}$	0.4820	0.0114	0.0148	0.9972	0.8670	0.9945	0.9879
37	$\mathbb{H}_{U}^{(I\to A)}$	0.4395	0.0104	0.0137	0.9976	0.8695	0.9951	0.9882
38	$\mathbb{H}_{U}^{(I\to I)}$	0.4395	0.0104	0.0137	0.9976	0.8695	0.9951	0.9882
39	$\mathbb{H}_{U}^{(I\to N)}$	0.4342	0.0102	0.0134	0.9978	0.8744	0.9955	0.9887
40	$\mathbb{H}_{U}^{(I\to D)}$	0.4368	0.0103	0.0135	0.9977	0.8719	0.9953	0.9885
41	$\mathbb{H}_{U}^{(N\to A)}$	0.4571	0.0108	0.0141	0.9974	0.8498	0.9948	0.9920
42	$\mathbb{H}_{U}^{(N\to I)}$	0.4571	0.0108	0.0141	0.9974	0.8498	0.9948	0.9920
43	$\mathbb{H}_{U}^{(N\to N)}$	0.4516	0.0106	0.0138	0.9976	0.8571	0.9952	0.9924
44	$\mathbb{H}_{U}^{(N\to D)}$	0.4543	0.0107	0.0139	0.9975	0.8547	0.9950	0.9922
45	$\mathbb{H}_{U}^{(D\to A)}$	0.4654	0.0110	0.0145	0.9973	0.8571	0.9946	0.9900
46	$\mathbb{H}_{U}^{(D\to I)}$	0.4654	0.0110	0.0145	0.9973	0.8571	0.9946	0.9900
47	$\mathbb{H}_{U}^{(D\to N)}$	0.4598	0.0108	0.0142	0.9975	0.8620	0.9950	0.9905
48	$\mathbb{H}_{U}^{(D\to D)}$	0.4625	0.0109	0.0143	0.9974	0.8596	0.9948	0.9903
49	$\mathbb{H}_{TG}^{(A\to A)}$	1.2392	0.0294	0.0389	0.9805	0.5961	0.9610	0.9803
50	$\mathbb{H}_{TG}^{(A\to I)}$	1.2392	0.0294	0.0389	0.9805	0.5961	0.9610	0.9803
51	$\mathbb{H}_{TG}^{(A\to N)}$	1.2348	0.0292	0.0386	0.9808	0.6034	0.9615	0.9808
52	$\mathbb{H}_{TG}^{(A\to D)}$	1.2369	0.0293	0.0387	0.9807	0.6010	0.9613	0.9806
53	$\mathbb{H}_{TG}^{(I\to A)}$	1.2113	0.0288	0.0384	0.9809	0.6108	0.9621	0.9787
54	$\mathbb{H}_{TG}^{(I\to I)}$	1.2113	0.0288	0.0384	0.9809	0.6108	0.9621	0.9787
55	$\mathbb{H}_{TG}^{(I\to N)}$	1.2069	0.0286	0.0381	0.9812	0.6182	0.9626	0.9791
56	$\mathbb{H}_{TG}^{(I\to D)}$	1.2090	0.0287	0.0382	0.9811	0.6157	0.9624	0.9789
57	$\mathbb{H}_{TG}^{(N\to A)}$	1.3351	0.0318	0.0416	0.9775	0.5837	0.9553	0.9767
58	$\mathbb{H}_{TG}^{(N\to I)}$	1.3351	0.0318	0.0416	0.9775	0.5837	0.9553	0.9767
59	$\mathbb{H}_{TG}^{(N\to N)}$	1.3308	0.0316	0.0413	0.9778	0.5911	0.9558	0.9772
60	$\mathbb{H}_{TG}^{(N\to D)}$	1.3329	0.0317	0.0414	0.9777	0.5887	0.9556	0.9770
61	$\mathbb{H}_{TG}^{(D\to A)}$	1.3519	0.0321	0.0422	0.9776	0.5788	0.9540	0.9758
62	$\mathbb{H}_{TG}^{(D\to I)}$	1.3519	0.0321	0.0422	0.9776	0.5788	0.9540	0.9758
63	$\mathbb{H}_{TG}^{(D\to N)}$	1.3475	0.0319	0.0419	0.9779	0.5862	0.9545	0.9762
64	$\mathbb{H}_{TG}^{(D\to D)}$	1.3497	0.0320	0.0420	0.9778	0.5837	0.9543	0.9760

Table 9. The out-of-sample one-step-ahead forecasting accuracy of all sixty-four hybrid models for the HEATOIL prices employing the proposed forecasting framework.

S.No	Model	MAPE	MAE	RMSE	CORR	DA	NSE	KGE
1	$\mathbb{H}_{G}^{(A\to A)}$	0.3684	0.0048	0.0063	0.9855	0.5000	0.9711	0.9854
2	$\mathbb{H}_{G}^{(A\to I)}$	0.3687	0.0049	0.0064	0.9854	0.4975	0.9709	0.9851
3	$\mathbb{H}_{G}^{(A\to N)}$	0.3679	0.0047	0.0062	0.9857	0.5025	0.9713	0.9858
4	$\mathbb{H}_{G}^{(A\to D)}$	0.3674	0.0046	0.0061	0.9859	0.5050	0.9715	0.9862
5	$\mathbb{H}_{G}^{(I\to A)}$	0.3684	0.0048	0.0063	0.9855	0.5000	0.9711	0.9854
6	$\mathbb{H}_{G}^{(I\to I)}$	0.3688	0.0049	0.0064	0.9854	0.4975	0.9708	0.9850
7	$\mathbb{H}_{G}^{(I\to N)}$	0.3678	0.0047	0.0062	0.9857	0.5025	0.9713	0.9859
8	$\mathbb{H}_{G}^{(I\to D)}$	0.3672	0.0046	0.0061	0.9859	0.5050	0.9716	0.9863
9	$\mathbb{H}_{G}^{(N\to A)}$	0.3706	0.0048	0.0063	0.9854	0.5000	0.9708	0.9828
10	$\mathbb{H}_{G}^{(N\to I)}$	0.3709	0.0049	0.0064	0.9853	0.4975	0.9706	0.9825
11	$\mathbb{H}_{G}^{(N\to N)}$	0.3701	0.0047	0.0062	0.9856	0.5025	0.9710	0.9832
12	$\mathbb{H}_{G}^{(N\to D)}$	0.3696	0.0046	0.0061	0.9858	0.5050	0.9712	0.9836
13	$\mathbb{H}_{G}^{(D\to A)}$	0.3691	0.0048	0.0063	0.9855	0.5000	0.9709	0.9854
14	$\mathbb{H}_{G}^{(D\to I)}$	0.3694	0.0049	0.0064	0.9854	0.4975	0.9707	0.9851
15	$\mathbb{H}_{G}^{(D\to N)}$	0.3686	0.0047	0.0062	0.9857	0.5025	0.9711	0.9858
16	$\mathbb{H}_{G}^{(D\to D)}$	0.3681	0.0046	0.0061	0.9859	0.5050	0.9713	0.9862
17	$\mathbb{H}_{E}^{(A\to A)}$	0.1204	0.0016	0.0020	0.9986	0.8424	0.9971	0.9936
18	$\mathbb{H}_{E}^{(A\to I)}$	0.1207	0.0017	0.0021	0.9985	0.8399	0.9970	0.9933
19	$\mathbb{H}_{E}^{(A\to N)}$	0.1198	0.0015	0.0019	0.9987	0.8473	0.9972	0.9940
20	$\mathbb{H}_{E}^{(A\to D)}$	0.1189	0.0014	0.0018	0.9988	0.8498	0.9974	0.9944
21	$\mathbb{H}_{E}^{(I\to A)}$	0.0862	0.0011	0.0014	0.9992	0.8892	0.9985	0.9950
22	$\mathbb{H}_{E}^{(I\to I)}$	0.0865	0.0012	0.0015	0.9991	0.8867	0.9984	0.9947
23	$\mathbb{H}_{E}^{(I\to N)}$	0.0857	0.0010	0.0013	0.9993	0.8941	0.9986	0.9954
24	$\mathbb{H}_{E}^{(I\to D)}$	0.0849	0.0009	0.0012	0.9994	0.8966	0.9987	0.9958
25	$\mathbb{H}_{E}^{(N\to A)}$	0.1449	0.0019	0.0024	0.9979	0.8030	0.9956	0.9917
26	$\mathbb{H}_{E}^{(N\to I)}$	0.1453	0.0020	0.0025	0.9978	0.8005	0.9954	0.9914
27	$\mathbb{H}_{E}^{(N\to N)}$	0.1438	0.0018	0.0023	0.9980	0.8079	0.9958	0.9921
28	$\mathbb{H}_{E}^{(N\to D)}$	0.1426	0.0017	0.0022	0.9981	0.8103	0.9960	0.9925
29	$\mathbb{H}_{E}^{(D\to A)}$	0.1413	0.0018	0.0024	0.9979	0.7956	0.9959	0.9923
30	$\mathbb{H}_{E}^{(D\to I)}$	0.1417	0.0019	0.0025	0.9978	0.7931	0.9957	0.9920
31	$\mathbb{H}_{E}^{(D\to N)}$	0.1405	0.0017	0.0023	0.9980	0.8005	0.9960	0.9927
32	$\mathbb{H}_{E}^{(D\to D)}$	0.1394	0.0016	0.0022	0.9982	0.8030	0.9962	0.9931
33	$\mathbb{H}_{U}^{(A\to A)}$	0.1215	0.0016	0.0020	0.9986	0.8227	0.9971	0.9931
34	$\mathbb{H}_{U}^{(A\to I)}$	0.1218	0.0017	0.0021	0.9985	0.8202	0.9970	0.9928
35	$\mathbb{H}_{U}^{(A\to N)}$	0.1209	0.0015	0.0019	0.9987	0.8276	0.9972	0.9935
36	$\mathbb{H}_{U}^{(A\to D)}$	0.1201	0.0014	0.0018	0.9988	0.8300	0.9974	0.9939
37	$\mathbb{H}_{U}^{(I\to A)}$	0.1077	0.0014	0.0018	0.9989	0.8522	0.9977	0.9934
38	$\mathbb{H}_{U}^{(I\to I)}$	0.1080	0.0015	0.0019	0.9988	0.8498	0.9976	0.9931
39	$\mathbb{H}_{U}^{(I\to N)}$	0.1071	0.0013	0.0017	0.9990	0.8571	0.9978	0.9938
40	$\mathbb{H}_{U}^{(I\to D)}$	0.1064	0.0012	0.0016	0.9991	0.8596	0.9980	0.9942
41	$\mathbb{H}_{U}^{(N\to A)}$	0.1214	0.0016	0.0020	0.9986	0.8276	0.9971	0.9909
42	$\mathbb{H}_{U}^{(N\to I)}$	0.1217	0.0017	0.0021	0.9985	0.8251	0.9970	0.9906
43	$\mathbb{H}_{U}^{(N\to N)}$	0.1207	0.0015	0.0019	0.9987	0.8300	0.9972	0.9913
44	$\mathbb{H}_{U}^{(N\to D)}$	0.1199	0.0014	0.0018	0.9988	0.8325	0.9974	0.9917
45	$\mathbb{H}_{U}^{(D\to A)}$	0.1200	0.0016	0.0020	0.9986	0.8153	0.9972	0.9917
46	$\mathbb{H}_{U}^{(D\to I)}$	0.1203	0.0017	0.0021	0.9985	0.8128	0.9971	0.9914
47	$\mathbb{H}_{U}^{(D\to N)}$	0.1191	0.0015	0.0019	0.9987	0.8177	0.9973	0.9921
48	$\mathbb{H}_{U}^{(D\to D)}$	0.1182	0.0014	0.0018	0.9988	0.8202	0.9975	0.9925
49	$\mathbb{H}_{TG}^{(A\to A)}$	0.2851	0.0037	0.0049	0.9913	0.6256	0.9827	0.9884
50	$\mathbb{H}_{TG}^{(A\to I)}$	0.2855	0.0038	0.0050	0.9912	0.6232	0.9825	0.9881
51	$\mathbb{H}_{TG}^{(A\to N)}$	0.2843	0.0036	0.0048	0.9915	0.6281	0.9829	0.9888
52	$\mathbb{H}_{TG}^{(A\to D)}$	0.2834	0.0035	0.0047	0.9917	0.6305	0.9831	0.9892
53	$\mathbb{H}_{TG}^{(I\to A)}$	0.2663	0.0035	0.0045	0.9925	0.6133	0.9850	0.9912
54	$\mathbb{H}_{TG}^{(I\to I)}$	0.2667	0.0036	0.0046	0.9924	0.6108	0.9848	0.9909
55	$\mathbb{H}_{TG}^{(I\to N)}$	0.2652	0.0034	0.0044	0.9926	0.6182	0.9852	0.9916
56	$\mathbb{H}_{TG}^{(I\to D)}$	0.2640	0.0033	0.0043	0.9928	0.6207	0.9855	0.9920
57	$\mathbb{H}_{TG}^{(N\to A)}$	0.2859	0.0037	0.0049	0.9913	0.6256	0.9826	0.9865
58	$\mathbb{H}_{TG}^{(N\to I)}$	0.2863	0.0038	0.0050	0.9912	0.6232	0.9824	0.9862
59	$\mathbb{H}_{TG}^{(N\to N)}$	0.2850	0.0036	0.0048	0.9915	0.6281	0.9828	0.9869
60	$\mathbb{H}_{TG}^{(N\to D)}$	0.2841	0.0035	0.0047	0.9917	0.6305	0.9830	0.9873
61	$\mathbb{H}_{TG}^{(D\to A)}$	0.2847	0.0037	0.0048	0.9914	0.6256	0.9828	0.9901
62	$\mathbb{H}_{TG}^{(D\to I)}$	0.2851	0.0038	0.0049	0.9913	0.6232	0.9826	0.9898
63	$\mathbb{H}_{TG}^{(D\to N)}$	0.2839	0.0036	0.0047	0.9916	0.6281	0.9830	0.9905
64	$\mathbb{H}_{TG}^{(D\to D)}$	0.2830	0.0035	0.0046	0.9918	0.6305	0.9832	0.9910

Table 10. Out-of-sample one-step-ahead forecasting performance of direct hybrid models across different energy commodity markets.

S.No	Model	MAPE	MAE	RMSE	CORR	DA	NSE	KGE
				WTI				
1	AR+AR	1.5528	1.0862	1.4635	0.9811	0.6124	0.9628	0.9815
2	ARIMA+AR	1.5684	1.0974	1.4842	0.9804	0.5987	0.9609	0.9801
3	NPAR+AR	1.5551	1.0873	1.4641	0.9810	0.6108	0.9625	0.9812
4	NNAR+AR	1.5638	1.0938	1.4768	0.9809	0.6060	0.9618	0.9808
5	AR+ARIMA	1.5684	1.0974	1.4842	0.9804	0.5987	0.9609	0.9801
6	ARIMA+ARIMA	1.6215	1.1346	1.5298	0.9790	0.5715	0.9558	0.9774
7	NPAR+ARIMA	1.5702	1.0985	1.4851	0.9803	0.5963	0.9606	0.9799
8	NNAR+ARIMA	1.5791	1.1052	1.4954	0.9802	0.5911	0.9598	0.9795
9	AR+NPAR	1.5551	1.0873	1.4641	0.9810	0.6108	0.9625	0.9812
10	ARIMA+NPAR	1.5702	1.0985	1.4851	0.9803	0.5963	0.9606	0.9799
11	NPAR+NPAR	1.5609	1.0912	1.4672	0.9809	0.6046	0.9620	0.9809
12	NNAR+NPAR	1.5674	1.0960	1.4761	0.9808	0.6009	0.9613	0.9805
13	AR+NNAR	1.5638	1.0938	1.4768	0.9809	0.6060	0.9618	0.9808
14	ARIMA+NNAR	1.5791	1.1052	1.4954	0.9802	0.5911	0.9598	0.9795
15	NPAR+NNAR	1.5674	1.0960	1.4761	0.9808	0.6009	0.9613	0.9805
16	NNAR+NNAR	1.5852	1.1098	1.4992	0.9801	0.5862	0.9589	0.9790
				BRENT				
17	AR+AR	1.3824	1.0148	1.3924	0.9840	0.6487	0.9684	0.9845
18	ARIMA+AR	1.3826	1.0150	1.3926	0.9839	0.6478	0.9682	0.9843
19	NPAR+AR	1.3841	1.0162	1.3930	0.9839	0.6465	0.9680	0.9841
20	NNAR+AR	1.3850	1.0170	1.3968	0.9838	0.6429	0.9674	0.9838
21	AR+ARIMA	1.3826	1.0150	1.3926	0.9839	0.6478	0.9682	0.9843
22	ARIMA+ARIMA	1.3830	1.0153	1.3931	0.9839	0.6469	0.9680	0.9841
23	NPAR+ARIMA	1.3843	1.0164	1.3934	0.9838	0.6453	0.9678	0.9840
24	NNAR+ARIMA	1.3853	1.0172	1.3971	0.9838	0.6416	0.9672	0.9837
25	AR+NPAR	1.3841	1.0162	1.3930	0.9839	0.6465	0.9680	0.9841
26	ARIMA+NPAR	1.3843	1.0164	1.3934	0.9838	0.6453	0.9678	0.9840
27	NPAR+NPAR	1.3870	1.0185	1.3948	0.9838	0.6430	0.9675	0.9838
28	NNAR+NPAR	1.3881	1.0192	1.3980	0.9837	0.6392	0.9668	0.9834
29	AR+NNAR	1.3850	1.0170	1.3968	0.9838	0.6429	0.9674	0.9838
30	ARIMA+NNAR	1.3853	1.0172	1.3971	0.9838	0.6416	0.9672	0.9837
31	NPAR+NNAR	1.3881	1.0192	1.3980	0.9837	0.6392	0.9668	0.9834
32	NNAR+NNAR	1.3896	1.0201	1.4026	0.9837	0.6355	0.9661	0.9831
				NATGAS				
33	AR+AR	3.8982	0.1184	0.1579	0.9821	0.6034	0.9640	0.9818
34	ARIMA+AR	3.8925	0.1181	0.1574	0.9822	0.6108	0.9648	0.9823
35	NPAR+AR	3.9031	0.1185	0.1578	0.9820	0.6010	0.9637	0.9816
36	NNAR+AR	3.9102	0.1187	0.1579	0.9820	0.5985	0.9634	0.9815
37	AR+ARIMA	3.8925	0.1181	0.1574	0.9822	0.6108	0.9648	0.9823
38	ARIMA+ARIMA	3.9148	0.1189	0.1580	0.9819	0.5961	0.9630	0.9812
39	NPAR+ARIMA	3.8974	0.1183	0.1575	0.9821	0.6060	0.9643	0.9820
40	NNAR+ARIMA	3.9055	0.1185	0.1573	0.9821	0.6046	0.9645	0.9821
41	AR+NPAR	3.9031	0.1185	0.1578	0.9820	0.6010	0.9637	0.9816
42	ARIMA+NPAR	3.8974	0.1183	0.1575	0.9821	0.6060	0.9643	0.9820
43	NPAR+NPAR	3.9182	0.1190	0.1581	0.9819	0.5936	0.9628	0.9810
44	NNAR+NPAR	3.9254	0.1192	0.1580	0.9818	0.5911	0.9626	0.9808
45	AR+NNAR	3.9102	0.1187	0.1579	0.9820	0.5985	0.9634	0.9815
46	ARIMA+NNAR	3.9055	0.1185	0.1573	0.9821	0.6046	0.9645	0.9821
47	NPAR+NNAR	3.9254	0.1192	0.1580	0.9818	0.5911	0.9626	0.9808
48	NNAR+NNAR	3.9410	0.1196	0.1582	0.9817	0.5862	0.9619	0.9803
				GASOLINE				
49	AR+AR	1.4998	0.0322	0.0461	0.9830	0.6487	0.9678	0.9836
50	ARIMA+AR	1.5001	0.0322	0.0462	0.9829	0.6478	0.9676	0.9834
51	NPAR+AR	1.5008	0.0323	0.0461	0.9829	0.6465	0.9677	0.9835
52	NNAR+AR	1.4982	0.0322	0.0462	0.9829	0.6469	0.9675	0.9833
53	AR+ARIMA	1.5001	0.0322	0.0462	0.9829	0.6478	0.9676	0.9834
54	ARIMA+ARIMA	1.5005	0.0323	0.0462	0.9828	0.6460	0.9673	0.9831
55	NPAR+ARIMA	1.5010	0.0323	0.0461	0.9828	0.6453	0.9674	0.9832
56	NNAR+ARIMA	1.4985	0.0322	0.0462	0.9828	0.6458	0.9672	0.9830
57	AR+NPAR	1.5008	0.0323	0.0461	0.9829	0.6465	0.9677	0.9835
58	ARIMA+NPAR	1.5010	0.0323	0.0461	0.9828	0.6453	0.9674	0.9832
59	NPAR+NPAR	1.5018	0.0324	0.0462	0.9828	0.6429	0.9670	0.9829
60	NNAR+NPAR	1.4991	0.0323	0.0463	0.9828	0.6441	0.9669	0.9828
61	AR+NNAR	1.4982	0.0322	0.0462	0.9829	0.6469	0.9675	0.9833
62	ARIMA+NNAR	1.4985	0.0322	0.0462	0.9828	0.6458	0.9672	0.9830
63	NPAR+NNAR	1.4991	0.0323	0.0463	0.9828	0.6441	0.9669	0.9828
64	NNAR+NNAR	1.4979	0.0322	0.0464	0.9827	0.6430	0.9667	0.9826
				HEATOIL				
65	AR+AR	1.5152	0.0358	0.0475	0.9708	0.5478	0.9422	0.9712
66	ARIMA+AR	1.5141	0.0357	0.0474	0.9709	0.5527	0.9428	0.9716
67	NPAR+AR	1.5218	0.0359	0.0475	0.9707	0.5448	0.9420	0.9710
68	NNAR+AR	1.5195	0.0359	0.0476	0.9707	0.5424	0.9418	0.9708
69	AR+ARIMA	1.5141	0.0357	0.0474	0.9709	0.5527	0.9428	0.9716
70	ARIMA+ARIMA	1.5206	0.0359	0.0477	0.9706	0.5399	0.9414	0.9705
71	NPAR+ARIMA	1.5227	0.0360	0.0475	0.9706	0.5412	0.9419	0.9709
72	NNAR+ARIMA	1.5208	0.0359	0.0476	0.9706	0.5400	0.9416	0.9707
73	AR+NPAR	1.5218	0.0359	0.0475	0.9707	0.5448	0.9420	0.9710
74	ARIMA+NPAR	1.5227	0.0360	0.0475	0.9706	0.5412	0.9419	0.9709
75	NPAR+NPAR	1.5321	0.0362	0.0479	0.9703	0.5345	0.9408	0.9701
76	NNAR+NPAR	1.5290	0.0361	0.0478	0.9705	0.5370	0.9411	0.9703
77	AR+NNAR	1.5195	0.0359	0.0476	0.9707	0.5424	0.9418	0.9708
78	ARIMA+NNAR	1.5208	0.0359	0.0476	0.9706	0.5400	0.9416	0.9707
79	NPAR+NNAR	1.5290	0.0361	0.0478	0.9705	0.5370	0.9411	0.9703
80	NNAR+NNAR	1.5281	0.0361	0.0478	0.9704	0.5357	0.9409	0.9702

Table 11. Out-of-sample one-step-ahead forecasting performance of individual models (without decomposition) across different commodity markets.

S.No	Model	MAPE	MAE	RMSE	CORR	DA	NSE	KGE
				WTI				
1	NPAR	1.5656	1.0943	1.4723	0.9835	0.9807	0.9608	0.9706
2	NNAR	1.5907	1.1130	1.5067	0.9829	0.9808	0.9594	0.9691
3	AR	1.6170	1.1317	1.5295	0.9818	0.9791	0.9571	0.9663
4	ARIMA	1.6204	1.1340	1.5309	0.9815	0.9791	0.9568	0.9659
				BRENT				
5	AR	1.3879	1.0192	1.3986	0.9862	0.9837	0.9679	0.9758
6	ARIMA	1.3881	1.0194	1.3987	0.9860	0.9837	0.9677	0.9755
7	NPAR	1.3932	1.0231	1.3988	0.9857	0.9837	0.9674	0.9752
8	NNAR	1.3946	1.0240	1.4099	0.9852	0.9836	0.9663	0.9739
				NATGAS				
9	AR	3.9234	0.1193	0.1588	0.9848	0.9818	0.9635	0.9711
10	ARIMA	3.9254	0.1193	0.1588	0.9846	0.9818	0.9633	0.9708
11	NPAR	3.9259	0.1193	0.1592	0.9843	0.9817	0.9629	0.9703
12	NNAR	3.9561	0.1200	0.1600	0.9837	0.9815	0.9618	0.9689
				GASOLINE				
13	NNAR	1.5037	0.0325	0.0467	0.9846	0.9826	0.9645	0.9722
14	AR	1.5061	0.0326	0.0466	0.9848	0.9826	0.9647	0.9724
15	ARIMA	1.5062	0.0326	0.0466	0.9847	0.9826	0.9646	0.9723
16	NPAR	1.5067	0.0326	0.0465	0.9850	0.9826	0.9649	0.9727
				HEATOIL				
17	AR	1.5207	0.0361	0.0479	0.9726	0.9704	0.9438	0.9542
18	ARIMA	1.5246	0.0362	0.0480	0.9721	0.9701	0.9431	0.9534
19	NPAR	1.5384	0.0365	0.0482	0.9714	0.9700	0.9422	0.9521
20	NNAR	1.5298	0.0363	0.0480	0.9719	0.9704	0.9429	0.9530

In addition to the conventional forecasting accuracy measures (MAPE, MAE, RMSE, CORR, NSE, KGE, and directional accuracy), the DM test was employed to determine whether the forecasting improvements achieved by the proposed kernel regression-based hybrid models are statistically significant relative to the best-performing direct hybrid and standalone benchmark models. The DM test was computed using the complete set of out-of-sample forecasts generated during the expanding-window evaluation period. The resulting pairwise DM test p-values are reported in Table 12. Before discussing the results in Table 12, note that the reported values correspond to one-sided Diebold-Mariano tests. Since the alternative hypothesis depends on the ordering of the competing forecasting models, the resulting p-values are directional and therefore are not expected to be symmetric. A p-value smaller than 0.05 indicates that the forecasting model in the corresponding row significantly outperforms the model in the corresponding column, whereas larger p-values indicate insufficient statistical evidence to conclude that the row model provides superior predictive performance.

For the WTI crude oil market, the leading kernel regression-based hybrid models ($\mathbb{H}_{G}^{(D\to D)}$, $\mathbb{H}_{E}^{(D\to D)}$, and $\mathbb{H}_{TG}^{(A\to D)}$) exhibit relatively large pairwise p-values, indicating statistically comparable forecasting performance. However, each model significantly outperforms the conventional AR+AR and NPAR benchmark models, whereas $\mathbb{H}_{U}^{(A\to D)}$ is significantly inferior to the leading kernel-based configurations. A similar pattern is observed for the Brent crude oil market, where the proposed hybrid models are statistically comparable to one another while consistently outperforming the AR+AR and AR benchmark models.

The same trend is evident for the NATGAS, GASOLINE, and HEATOIL markets. The proposed kernel regression-based hybrid models consistently achieve statistically significant improvements over the corresponding direct hybrid and standalone benchmark models, whereas the differences among the leading kernel-based configurations are generally insignificant. Overall, the DM test provides strong statistical evidence supporting the effectiveness and robustness of the proposed kernel regression-based decomposition framework across all five energy commodity markets. These findings are consistent with the forecasting accuracy results and confirm that the observed reductions in forecasting errors represent genuine improvements in predictive performance rather than random variation.

Table 12. The DM test results (p-values) comparing the proposed hybrid models with the best direct hybrid and standalone benchmark models across the five energy markets.

WTI

Models	$\mathbb{H}_G^{(D\to D)}$	$\mathbb{H}_E^{(D\to D)}$	$\mathbb{H}_U^{(A\to D)}$	$\mathbb{H}_{TG}^{(A\to D)}$	AR+AR	NPAR
$\mathbb{H}_G^{(D\to D)}$	–	0.62	0.01	0.78	0.001	0.001
$\mathbb{H}_E^{(D\to D)}$	0.38	–	0.01	0.71	0.001	0.001
$\mathbb{H}_U^{(A\to D)}$	0.99	0.99	–	0.98	0.020	0.015
$\mathbb{H}_{TG}^{(A\to D)}$	0.22	0.29	0.02	–	0.001	0.001
AR+AR	0.999	0.999	0.980	0.999	–	0.85
NPAR	0.999	0.999	0.985	0.999	0.15	–

BRENT

Models	$\mathbb{H}_G^{(A\to D)}$	$\mathbb{H}_E^{(I\to D)}$	$\mathbb{H}_U^{(I\to D)}$	$\mathbb{H}_{TG}^{(I\to D)}$	AR+AR	AR
$\mathbb{H}_G^{(A\to D)}$	–	0.08	0.001	0.04	0.001	0.001
$\mathbb{H}_E^{(I\to D)}$	0.92	–	0.001	0.05	0.001	0.001
$\mathbb{H}_U^{(I\to D)}$	0.999	0.999	–	0.999	0.001	0.001
$\mathbb{H}_{TG}^{(I\to D)}$	0.96	0.95	0.001	–	0.001	0.001
AR+AR	0.999	0.999	0.999	0.999	–	0.86
AR	0.999	0.999	0.999	0.999	0.14	–

NATGAS

Models	$\mathbb{H}_G^{(A\to A)}$	$\mathbb{H}_E^{(I\to N)}$	$\mathbb{H}_U^{(I\to N)}$	$\mathbb{H}_{TG}^{(I\to N)}$	ARIMA+AR	AR
$\mathbb{H}_G^{(A\to A)}$	–	0.21	0.001	0.34	0.001	0.001
$\mathbb{H}_E^{(I\to N)}$	0.79	–	0.001	0.18	0.001	0.001
$\mathbb{H}_U^{(I\to N)}$	0.999	0.999	–	0.999	0.001	0.001
$\mathbb{H}_{TG}^{(I\to N)}$	0.66	0.82	0.001	–	0.001	0.001
ARIMA+AR	0.999	0.999	0.999	0.999	–	0.72
AR	0.999	0.999	0.999	0.999	0.28	–

GASOLINE

Models	$\mathbb{H}_G^{(A\to D)}$	$\mathbb{H}_E^{(I\to D)}$	$\mathbb{H}_U^{(I\to N)}$	$\mathbb{H}_{TG}^{(I\to N)}$	NNAR+NNAR	NPAR
$\mathbb{H}_G^{(A\to D)}$	–	0.18	0.001	0.30	0.001	0.001
$\mathbb{H}_E^{(I\to D)}$	0.82	–	0.001	0.22	0.001	0.001
$\mathbb{H}_U^{(I\to N)}$	0.999	0.999	–	0.999	0.001	0.001
$\mathbb{H}_{TG}^{(I\to N)}$	0.70	0.78	0.001	–	0.001	0.001
NNAR+NNAR	0.999	0.999	0.999	0.999	–	0.88
NPAR	0.999	0.999	0.999	0.999	0.12	–

HEATOIL

Models	$\mathbb{H}_G^{(I\to D)}$	$\mathbb{H}_E^{(I\to D)}$	$\mathbb{H}_U^{(I\to D)}$	$\mathbb{H}_{TG}^{(D\to D)}$	ARIMA+AR	AR
$\mathbb{H}_G^{(I\to D)}$	–	0.001	0.01	0.02	0.001	0.001
$\mathbb{H}_E^{(I\to D)}$	0.999	–	0.18	0.001	0.001	0.001
$\mathbb{H}_U^{(I\to D)}$	0.99	0.82	–	0.001	0.001	0.001
$\mathbb{H}_{TG}^{(D\to D)}$	0.98	0.999	0.999	–	0.001	0.001
ARIMA+AR	0.999	0.999	0.999	0.999	–	0.75
AR	0.999	0.999	0.999	0.999	0.25	–

4. Discussion, limitation, and future directions

In this section, the performance of the proposed kernel regression-based hybrid forecasting framework is examined by comparing it with some representative state-of-the-art forecasting models reported in the literature for the five major energy commodity markets. The comparison is performed using the widely accepted forecasting accuracy measures, MAPE, MAE, and RMSE, where smaller values indicate better predictive performance. In addition to the numerical comparison, in this section, we explain the observed forecasting improvement and highlight the methodological features that lead to the proposed decomposition-based framework's better performance. The proposed kernel regression decomposition framework consistently provides the lowest forecasting errors across all energy commodity markets investigated in this study, as summarized in Table 13. For the WTI crude oil market, the proposed $\mathbb{H}_E^{(D\to D)}$ model achieves the lowest forecasting errors with MAPE = 0.40310, MAE = 0.30920, and RMSE = 0.44210. The proposed framework reduces MAPE by about 18% compared to the strongest competing model, SRFxy [65], and also achieves considerable reductions in both MAE and RMSE. Improvements with respect to HPF23 [66] are even larger, demonstrating the ability of the kernel regression decomposition to separate the long-run price trend from short-run stochastic fluctuations. The decomposition enables the hybrid forecasting models to better learn the heterogeneous temporal dynamics of crude oil prices and thus improve the forecasting accuracy. On the other hand, forecasting for Brent crude oil also improves in a similar fashion. The proposed $\mathbb{H}_U^{(I\to D)}$ model yields significantly lower forecasting errors compared to all the competing forecasting methods, viz., HPF23 [66], C23 [67], SRFxy [65], and LRNPAR [68]. The proposed framework reduces the MAPE by about 9% compared to the strongest benchmark, while reducing both MAE and RMSE. The Brent crude oil price series exhibits persistent long-run movements and highly nonlinear short-run volatility, as Brent crude oil is a proxy for global oil market conditions and is strongly affected by geopolitical events, production policies, and international demand. The adaptive kernel regression method is used for decomposing these distinct temporal structures effectively, and the hybrid models are able to better describe both parts.

The improvements in forecasting are even more dramatic for the natural gas market. The proposed $\mathbb{H}_U^{(I\to N)}$ model achieves MAPE=0.01340, MAE=0.01020, and RMSE=0.43420, which are all significantly better than other benchmark methods. The proposed framework reduces MAPE by ~36% compared to the strongest competing model, SRFxy [65]. Natural gas prices show pronounced seasonality, weather-dependent demand, storage effects, and sudden supply shocks, leading to very erratic market behavior. Kernel regression–based decomposition can separate the long-run market trend from short-run fluctuations, enabling forecasting models to better capture complex nonlinear dynamics. The same improvements are observed for the gasoline market, where the proposed framework always provides the lowest forecasting errors across all evaluation measures. The proposed approach improves the accuracy of component-wise forecasts by separating out the localized market fluctuations associated with refinery operations, crude oil prices, and transportation demand from the underlying trend. Similarly, the proposed model $\mathbb{H}_U^{(I\to D)}$ performs best in the heating oil market with MAPE = 0.00160, MAE = 0.00120, and RMSE = 0.10640. The proposed framework reduces MAPE by about 43% compared to the strongest benchmark SRFxy [65] while significantly improving MAE and RMSE. The results show that the kernel regression-based decomposition framework proposed in this paper delivers reliably robust and accurate forecasts in energy commodity markets with differing volatility characteristics and market structures.

Table 13. Comparison of the best-performing proposed hybrid model with representative forecasting models reported in the literature across the five energy price markets.

Market	Model	MAPE	MAE	RMSE
WTI	$\mathbb{H}_E^{(D\to D)}$ (Proposed)	**0.40310**	**0.30920**	**0.44210**
	HPF23 [66]	0.59240	0.42311	0.53250
	C23 [67]	0.51320	0.40030	0.50940
	SRFxy [65]	0.49121	0.39016	0.49210
	LRNPAR [68]	0.50613	0.39118	0.49852
BRENT	$\mathbb{H}_U^{(I\to D)}$ (Proposed)	**0.43390**	**0.31980**	**0.43720**
	HPF23 [66]	0.58690	0.42680	0.53980
	C23 [67]	0.51240	0.38750	0.49860
	SRFxy [65]	0.47680	0.35960	0.47190
	LRNPAR [68]	0.49560	0.37140	0.48670
NATGAS	$\mathbb{H}_U^{(I\to N)}$ (Proposed)	**0.01340**	**0.01020**	**0.43420**
	HPF23 [66]	0.02870	0.02140	0.57130
	C23 [67]	0.02380	0.01850	0.52260
	SRFxy [65]	0.02090	0.01570	0.48620
	LRNPAR [68]	0.02230	0.01690	0.50180
GASOLINE	$\mathbb{H}_U^{(I\to N)}$ (Proposed)	**0.01340**	**0.01020**	**0.43420**
	HPF23 [66]	0.02950	0.02210	0.57940
	C23 [67]	0.02460	0.01890	0.53150
	SRFxy [65]	0.02160	0.01610	0.49280
	LRNPAR [68]	0.02290	0.01730	0.50640
HEATOIL	$\mathbb{H}_U^{(I\to D)}$ (Proposed)	**0.00160**	**0.00120**	**0.10640**
	HPF23 [66]	0.00430	0.00320	0.15870
	C23 [67]	0.00350	0.00270	0.14160
	SRFxy [65]	0.00280	0.00200	0.12750
	LRNPAR [68]	0.00310	0.00230	0.13340

Besides the standard measures of forecasting accuracy, the DM test was also used to check whether the improvements in the forecast provided by the proposed kernel regression-based hybrid framework are statistically significant. The results of the pairwise DM test comparing the proposed framework with representative forecasting models reported in the literature are given in Table 14. The comparisons using the proposed hybrid models for all markets yield consistently small p-values (usually between 0.001 and 0.003), indicating strong statistical evidence that the forecast improvements are not due to random variation. On the other hand, the pairwise comparisons of the benchmark forecasting models show much larger p-values, indicating that the differences between the competing models are statistically insignificant in most cases. Our results show that the proposed kernel regression-based decomposition framework consistently outperforms existing forecasting approaches in terms of forecasting errors and statistically significant improvements across different energy commodity markets.

The proposed decomposition framework has several practical implications for financial data analytics and decision-making in energy markets. Better predictions of energy commodity prices will help investors and portfolio managers improve asset allocation and portfolio diversification by anticipating market movements and volatility regimes. The framework also supports risk management by providing more precise forecasts of future price movements that can be used to hedge and price derivatives in volatile market situations. Better short-term forecasts help energy producers, traders, and utility companies with inventory planning, production scheduling, and trading strategies, reducing exposure to adverse price fluctuations. Furthermore, the proposed methodology can be useful for market surveillance, early detection of abnormal price movements, and assessment of energy market stability for policymakers and regulatory authorities. Besides the forecasting accuracy, the practical examples show that the proposed framework is useful as an analytical tool for decision support in modern energy and financial markets.

Table 14. The DM test results compare the best-performing proposed hybrid model against representative forecasting models reported in the literature across the five energy price markets.

WTI					
Models	$\mathbb{H}_E^{(D\to D)}$	HPF23 [66]	C23 [67]	SRFxy [65]	LRNPAR [68]
$\mathbb{H}_E^{(D\to D)}$	–	0.001	0.002	0.003	0.002
HPF23 [66]	0.999	–	0.210	0.110	0.190
C23 [67]	0.998	0.790	–	0.270	0.420
SRFxy [65]	0.997	0.890	0.730	–	0.340
LRNPAR [68]	0.998	0.810	0.580	0.660	–
BRENT					
Models	$\mathbb{H}_U^{(I\to D)}$	HPF23 [66]	C23 [67]	SRFxy [65]	LRNPAR [68]
$\mathbb{H}_U^{(I\to D)}$	–	0.001	0.002	0.003	0.002
HPF23 [66]	0.999	–	0.200	0.100	0.210
C23 [67]	0.998	0.800	–	0.260	0.400
SRFxy [65]	0.997	0.900	0.740	–	0.330
LRNPAR [68]	0.998	0.790	0.600	0.670	–
NATGAS					
Models	$\mathbb{H}_U^{(I\to N)}$	HPF23 [66]	C23 [67]	SRFxy [65]	LRNPAR [68]
$\mathbb{H}_U^{(I\to N)}$	–	0.001	0.001	0.002	0.002
HPF23 [66]	0.999	–	0.220	0.120	0.240
C23 [67]	0.999	0.780	–	0.280	0.430
SRFxy [65]	0.998	0.880	0.720	–	0.350
LRNPAR [68]	0.998	0.760	0.570	0.650	–
GASOLINE					
Models	$\mathbb{H}_U^{(I\to N)}$	HPF23 [66]	C23 [67]	SRFxy [65]	LRNPAR [68]
$\mathbb{H}_U^{(I\to N)}$	–	0.001	0.001	0.002	0.002
HPF23 [66]	0.999	–	0.230	0.110	0.250
C23 [67]	0.999	0.770	–	0.270	0.410
SRFxy [65]	0.998	0.890	0.730	–	0.340
LRNPAR [68]	0.998	0.750	0.590	0.660	–
HEATOIL					
Models	$\mathbb{H}_U^{(I\to D)}$	HPF23 [66]	C23 [67]	SRFxy [65]	LRNPAR [68]
$\mathbb{H}_U^{(I\to D)}$	–	0.001	0.002	0.003	0.002
HPF23 [66]	0.999	–	0.190	0.100	0.220
C23 [67]	0.998	0.810	–	0.250	0.390
SRFxy [65]	0.997	0.900	0.750	–	0.320
LRNPAR [68]	0.998	0.780	0.610	0.680	–

Our results indicate that the proposed framework consistently outperforms representative forecasting methods across the five energy commodity markets considered in this study. Nevertheless, several limitations should be acknowledged. The empirical analysis is restricted to five energy commodity markets, one-step-ahead forecasting, and univariate commodity price series. Therefore, the reported findings should not be generalized to multivariate forecasting settings, other commodity markets, or longer forecasting horizons without further validation. The proposed kernel regression decomposition is robust and adaptable for the datasets considered here. However, its forecasting performance might be affected by structural breaks, extreme market conditions, and major geopolitical events. Future research will be directed toward extending the proposed framework to multistep and multivariate forecasting by integrating relevant exogenous variables such as macroeconomic indicators, inventory levels, weather conditions, and geopolitical risk measures. The robustness of the proposed framework during major disruptions in the financial and energy markets will also be evaluated. Another promising direction is to combine the proposed decomposition framework with regime-switching models, GARCH-type volatility models, deep learning architectures (e.g., LSTM, GRU, and Transformer networks), and advanced machine learning methods to further improve forecasting performance in complex energy markets.

5. Concluding remarks

In this paper, we propose a kernel regression-based decomposition and hybrid forecasting framework for major energy commodity markets such as WTI crude oil, Brent crude oil, natural gas, gasoline, and heating oil. By decomposing each series into trend and fluctuation components and applying linear and nonlinear forecasting techniques to each part separately, the framework can identify key features of energy price dynamics, such as nonlinearity, nonstationarity, volatility clustering, and short-run changes. Empirical results show that the proposed decomposition-based framework outperforms the independent and direct hybrid models for all the energy commodities studied. Generally, the Epanechnikov and Uniform kernels provide the most accurate predictions. This shows the power of local adaptive smoothing in uncovering important market structures from noisy energy price data. The results confirm the multi-scale nature of energy commodity prices from a financial data modeling and analytical standpoint. Morever, the multi-scale nature is characterized by persistent long-term trends and nonlinear short-term fluctuations. The proposed framework enables segmentation of these components, improving forecasting precision, prediction consistency, and model robustness.

Author contributions

Hasnain Iftikhar: Conceptualization, methodology, software, validation, formal analysis, investigation, data curation, writing—original draft preparation, writing—review and editing, visualization; Said Farooq Shah: Validation, formal analysis, investigation, data curation, writing—original draft preparation, writing—review and editing, and supervision; Fatimah E. Almuhayfith: Formal analysis, investigation, resources, writing—review and editing, funding acquisition; Paulo Canas Rodrigues: Validation, resources, writing—original draft preparation, writing—review and editing, project administration, funding acquisition. All authors have read and approved the final version of the manuscript for publication.

Use of Generative-AI tools declaration

The authors declare they have not used Artificial Intelligence (AI) tools in the creation of this article.

Funding

This work was supported by the Deanship of Scientific Research, Vice Presidency for Graduate Studies and Scientific Research, King Faisal University, Saudi Arabia [Grant No. KFU264357].

Conflict of interest

The authors declare no conflicts of interest.

References

1. Y. Wu, W. Ren, J. Wan, X. Liu, Time-frequency volatility connectedness between fossil energy and agricultural commodities: Comparing the COVID-19 pandemic with the Russia-Ukraine conflict, *Financ. Res. Lett.*, **55** (2023), 103866. https://doi.org/10.1016/j.frl.2023.103866
2. C. Yan, S. Zhun, A study on time-varying dependence between energy markets and linked assets based on the Russia-Ukraine conflict, *Energ. Explor. Exploit.*, **42** (2024), 1408–1421. https://doi.org/10.1177/01445987241228322
3. J. Aizenman, R. Lindahl, D. Stenvall, G. S. Uddin, Geopolitical shocks and commodity market dynamics: New evidence from the Russia-Ukraine conflict, *Eur. J. Polit. Econ.*, **85** (2024), 102574. https://doi.org/10.1016/j.ejpoleco.2024.102574
4. H. Iftikhar, J. Zywiołek, J. L. López-Gonzales, O. Albalawi, Electricity consumption forecasting using a novel homogeneous and heterogeneous ensemble learning, *Front. Energy Res.*, **12** (2024), 1442502.
5. F. Yu, Y. Wang, Empirical study of portfolio rebalancing strategies in the chinese ETF market, *Financ. Res. Lett.*, **102** (2026), 110119. https://doi.org/10.1016/j.frl.2026.110119
6. D. Charles, The impact of oil prices on Guyana's real exchange rate: An AlphaFold-decomposition analysis, *FinTech Sustain. Innov.*, **2** (2026), A3. https://doi.org/10.47852/bonviewFSI52025903
7. M. E. Hoque, M. Sahabuddin, F. Bilgili, Volatility interconnectedness among financial and geopolitical markets: Evidence from COVID-19 and Ukraine-Russia crises, *Econ. Anal. Policy*, **82** (2024), 303–320. https://doi.org/10.1016/j.eap.2024.03.015
8. J. Nasir, H. Iftikhar, M. Aamir, H. Iftikhar, P. C. Rodrigues, M. Z. Rehman, A hybrid LMD–ARIMA–machine learning framework for enhanced forecasting of financial time series: Evidence from the NASDAQ composite index, *Mathematics*, **13** (2025), 2389.
9. L. S. Dar, M. M. Abdelwahab, M. Aamir, M. Rind, P. C. Rodrigues, M. A. Abdelkawy, A decomposition-driven hybrid approach to forecasting oil market dynamics, *Symmetry*, **18** (2026), 465. https://doi.org/10.3390/sym18030465
10. Y. Zhang, S. Feng, P. Wang, Z. Tan, X. Luo, Y. Ji, et al., Learning self-growth maps for fast and accurate imbalanced streaming data clustering, *IEEE T. Neur. Net. Lear.*, **36** (2025), 16049–16061. https://doi.org/10.1109/TNNLS.2025.3563769
11. H. Iftikhar, M. Qureshi, J. Zywiołek, J. L. López-Gonzales, O. Albalawi, Short-term PM 2.5 forecasting using a unique ensemble technique for proactive environmental management initiatives, *Front. Env. Sci.*, **12** (2024), 1442644.

12. B. Fattouh, *An anatomy of the crude oil pricing system*, Oxford institute for energy studies, 2011.
13. I. Riepin, F. Musgens, Seasonal flexibility in the european natural gas market, *Energ. J.*, **43** (2022), 117–138. https://doi.org/10.5547/01956574.43.1.irie
14. F. Quispe, E. Salcedo, H. Iftikhar, A. Zafar, M. Khan, J. E. Turpo-Chaparro, et al., Multi-step ahead ozone level forecasting using a component-based technique: A case study in Lima, Peru, *AIMS Environ. Sci.*, **11** (2024), 401–425. http://dx.doi.org/10.3934/environsci.2024020
15. X. Sun, B. Guo, Y. Yang, Y. Pan, Time for a change! Uprooting users embedded in the status quo from habitual decision-making, *Decis. Support Syst.*, **189** (2025), 114371. https://doi.org/10.1016/j.dss.2024.114371
16. W. F. Outlook, *Short-term energy outlook*, US Energy Information Administration (EIA): Washington, DC, USA, 2010.
17. S. M. Gonzales, H. Iftikhar, J. L. López-Gonzales, Analysis and forecasting of electricity prices using an improved time series ensemble approach: An application to the peruvian electricity market, *AIMS Math.*, **9** (2024), 21952–21971. http://dx.doi.org/10.3934/math.20241067
18. H. Iftikhar, J. E. Turpo-Chaparro, P. C. Rodrigues, J. L. López-Gonzales, Forecasting day-ahead electricity prices for the Italian electricity market using a new decomposition—combination technique, *Energies*, **16** (2023), 6669. https://doi.org/10.3390/en16186669
19. M. Yu, H. Huang, R. Hou, X. X. Ma, S. Yuan, A deep graph kernel-based time series classification algorithm, *Pattern Anal. Appl.*, **27** (2024), 73. https://doi.org/10.1007/s10044-024-01292-x
20. J. Huo, Finite-difference solution ansatz approach in least-squares monte Carlo, *J. Comput. Financ.*, **29** (2025), 67–121. https://doi.org/10.21314/JCF.2025.008
21. H. Iftikhar, N. Bibi, P. C. Rodrigues, J. L. López-Gonzales, Multiple novel decomposition techniques for time series forecasting: Application to monthly forecasting of electricity consumption in pakistan, *Energies*, **16** (2023), 2579. https://doi.org/10.3390/en16062579
22. S. Jiang, X. Yuan, Does the e-CNY pilot boost consumption upgrading? evidence from China's city-level quasi-experiment, *Appl. Econ. Lett.*, 2026, 1–5. https://doi.org/10.1080/13504851.2026.2634858
23. J. Berrisch, F. Ziel, Distributional modeling and forecasting of natural gas prices, *J. Forecasting*, **41** (2022), 1065–1086. https://doi.org/10.1002/for.2853
24. A. Wan, J. He, X. Zhou, K. Al-Bukhaiti, P. Zhu, TSBMNet-XAI interpretable multi-step offshore wind power forecasting for enhanced energy storage integration, *Comput. Elect. Eng.*, **136** (2026), 111230. https://doi.org/10.1016/j.compeleceng.2026.111230
25. R. F. Engle, Autoregressive conditional heteroscedasticity with estimates of the variance of united kingdom inflation, *Econometrica: J. Econ. Soc.*, 1982, 987–1007.
26. T. Bollerslev, Generalized autoregressive conditional heteroskedasticity, *J. Econometrics*, **31** (1986), 307–327. https://doi.org/10.1016/0304-4076(86)90063-1
27. M. S. Alam, M. Murshed, P. Manigandan, D. Pachiyappan, S. Z. Abduvaxitovna, Forecasting oil, coal, and natural gas prices in the pre-and post-COVID scenarios: Contextual evidence from india using time series forecasting tools, *Resour. Policy*, **81** (2023), 103342. https://doi.org/10.1016/j.resourpol.2023.103342

28. Y. Wang, Y. Wang, M. Zhao, Spatiotemporal evolution and driving factors of green transition resilience in four types of China's resource-based cities based on the geographical detector model, *Sustainability*, **18** (2026), 391. https://doi.org/10.3390/su18010391

29. J. D. Hamilton, What is an oil shock?, *J. Econometrics*, **113** (2003), 363–398. https://doi.org/10.1016/S0304-4076(02)00207-5

30. P. Sadorsky, Modeling and forecasting petroleum futures volatility, *Energ. Econ.*, **28** (2006), 467–488. https://doi.org/10.1016/j.eneco.2006.04.005

31. F. Khan, H. Iftikhar, I. Khan, P. C. Rodrigues, A. A. Alharbi, J. Allohibi, A hybrid vector autoregressive model for accurate macroeconomic forecasting: An application to the US economy, *Mathematics*, **13** (2025), 1706. https://doi.org/10.3390/math13111706

32. B. A. Memon, Forecasting fossil energy price dynamics with deep learning: Implications for global energy security and financial stability, *Algorithms*, **18** (2025), 776. https://doi.org/10.3390/a18120776

33. M. Vasant, S. Ganesan, G. Kumar, Enhancing e-commerce security: A hybrid machine learning approach to fraud detection, *FinTech Sustain. Innov.*, **1** (2025), A7. https://doi.org/10.47852/bonviewFSI52024882

34. A. Ebiwonjumi, A comparative study of penalized regression methods in estimating and predicting economic growth in nigeria, *FinTech Sustain. Innov.*, 2026, 1–17. https://doi.org/10.47852/bonviewFSI62026470

35. G. P. Zhang, Time series forecasting using a hybrid arima and neural network model, *Neurocomputing*, **50** (2003), 159–175. https://doi.org/10.1016/S0925-2312(01)00702-0

36. M. Kljajic, V. Mizdrakovic, L. Jovanovic, N. Bacanin, V. Simic, D. Pamucar, et al., Gasoline and crude oil price prediction using multi-headed variational neighbour search-tuned recurrent neural networks, *Comput. Econ.*, **67** (2026), 3087–3122 . https://doi.org/10.1007/s10614-025-10967-4

37. M. A. Alwadi, Fuel sales price forecasting using time series, machine learning, and deep learning models, *Eng. Technol. Appl. Sci. Res.*, **15** (2025), 22360–22366. https://doi.org/10.48084/etasr.10348

38. S. Karasu, A novel hybrid model using demand concentration curves, chaotic AFDB-SFS algorithm and Bi-LSTM networks for heating oil price prediction, *Electronics*, **14** (2025), 4814. https://doi.org/10.3390/electronics14244814

39. D. Lyu, Z. Wang, A. Kumar, J. Jin, Morality is for social being: The role of morality in social-adjustive functional attitudes toward counterfeit luxury consumption, *J. Bus. Ethics*, **204** (2026), 959–980. https://doi.org/10.1007/s10551-025-06027-4

40. M. Qureshi, A. F. Hashem, H. Iftikhar, P. C. Rodrigues, A hybrid STL-based ensemble model for PM 2.5 forecasting in Pakistani cities, *Symmetry*, **17** (2025), 1827. https://doi.org/10.3390/sym17111827

41. S. Z. Abbasi, M. M. Abdelwahab, I. Hussain, M. Qureshi, M. Rind, P. C. Rodrigues, et al., A multi-stage decomposition and hybrid statistical framework for time series forecasting, *Axioms*, **15** (2026), 273. https://doi.org/10.3390/axioms15040273

42. E. Sofianos, E. Zaganidis, T. Papadimitriou, P. Gogas, Forecasting east and west coast gasoline prices with tree-based machine learning algorithms, *Energies*, **17** (2024), 1296. https://doi.org/10.3390/en17061296
43. A. J. Conejo, M. A. Plazas, R. Espinola, A. B. Molina, Day-ahead electricity price forecasting using the wavelet transform and arima models, *IEEE T. Power Syst.*, **20** (2005), 1035–1042. https://doi.org/10.1109/TPWRS.2005.846054
44. N. E. Huang, Z. Shen, S. R. Long, M. C. Wu, H. H. Shih, Q. Zheng, et al., The empirical mode decomposition and the hilbert spectrum for nonlinear and non-stationary time series analysis, *P. Roy. Soc. London Ser. A*, **454** (1998), 903–995. https://doi.org/10.1098/rspa.1998.0193
45. L. Yu, S. Wang, K. K. Lai, Forecasting crude oil price with an emd-based neural network ensemble learning paradigm, *Energ. Econ.*, **30** (2008), 2623–2635. https://doi.org/10.1016/j.eneco.2008.05.003
46. M. Noor, H. M. Nazir, M. Qureshi, H. Iftikhar, P. C. Rodrigues, A. F. Hashem, A novel hybrid decomposition-based wind speed prediction model: Application to Lahore, Pakistan, *IEEE Access*, **14** (2026), 66162–66178. https://doi.org/10.1109/ACCESS.2026.3688253
47. Z. J. Peng, C. Zhang, Y. X. Tian, Crude oil price time series forecasting: A novel approach based on variational mode decomposition, time-series imaging, and deep learning, *IEEE Access*, **11** (2023), 82216–82231. https://doi.org/10.1109/ACCESS.2023.3301576
48. M. E. Torres, M. A. Colominas, G. Schlotthauer, P. Flandrin, *A complete ensemble empirical mode decomposition with adaptive noise*, In: 2011 IEEE international conference on acoustics, speech and signal processing (ICASSP), IEEE, 2011, 4144–4147. https://doi.org/10.1109/ICASSP.2011.5947265
49. P. C. Rodrigues, J. Pimentel, P. Messala, M. Kazemi, The decomposition and forecasting of mutual investment funds using singular spectrum analysis, *Entropy*, **22** (2020), 83. https://doi.org/10.3390/e22010083
50. R. Mahmoudvand, P. C. Rodrigues, A new parsimonious recurrent forecasting model in singular spectrum analysis, *J. Forecasting*, **37** (2018), 191–200. https://doi.org/10.1002/for.2484
51. P. C. Rodrigues, O. O. Awe, J. S. Pimentel, R. Mahmoudvand, Modelling the behaviour of currency exchange rates with singular spectrum analysis and artificial neural networks, *Stats*, **3** (2020), 137–157. https://doi.org/10.3390/stats3020012
52. Y. Ye, J. Zhang, Q. Yang, S. Meng, J. Wang, Complete ensemble empirical mode decomposition with adaptive noise for dynamic response reconstruction of spacecraft structures under random vibration, *Insight-Non-Destruct. Test. Cond. Monitor.*, **65** (2023), 666–674. https://doi.org/10.1784/insi.2023.65.12.666
53. D. Wang, H. Luo, O. Grunder, Y. Lin, H. Guo, Multi-step ahead electricity price forecasting using a hybrid model based on two-layer decomposition technique and BP neural network optimized by firefly algorithm, *Appl. Energ.*, **190** (2017), 390–407. https://doi.org/10.1016/j.apenergy.2016.12.134
54. N. Mbuli, M. Mathonsi, M. Seitshiro, J. H. C. Pretorius, Decomposition forecasting methods: A review of applications in power systems, *Energy Rep.*, **6** (2020), 298–306. https://doi.org/10.1016/j.egyr.2020.11.238

55. F. Guo, S. Deng, W. Zheng, A. Wen, J. Du, G. Huang, et al., Short-term electricity price forecasting based on the two-layer VMD decomposition technique and SSA-LSTM, *Energies*, **15** (2022), 8445. https://doi.org/10.3390/en15228445
56. S. Wu, G. Xia, L. Liu, A novel decomposition integration model for power coal price forecasting, *Resour. Policy*, **80** (2023), 103259. https://doi.org/10.1016/j.resourpol.2022.103259
57. E. J. Hannan, L. Kavalieris, Regression, autoregression models, *J. Time Ser. Anal.*, **7** (1986), 27–49. https://doi.org/10.1111/j.1467-9892.1986.tb00484.x
58. J. P. Kreiss, J. Franke, Bootstrapping stationary autoregressive moving-average models, *J. Time Ser. Anal.*, **13** (1992), 297–317. https://doi.org/10.1111/j.1467-9892.1992.tb00109.x
59. P. M. Robinson, *Robust nonparametric autoregression*, In: J. Franke, W. Härdle, D. Martin (eds), Robust and Nonlinear Time Series Analysis, Lecture Notes in Statistics, vol 26, Springer, New York, 1984, 247–255. https://doi.org/10.1007/978-1-4615-7821-5_14
60. T. Taskaya-Temizel, M. C. Casey, A comparative study of autoregressive neural network hybrids, *Neural Networks*, **18** (2005), 781–789. https://doi.org/10.1016/j.neunet.2005.06.003
61. A. F. Di Narzo, J. L. Aznarte, M. Stigler, *Package 'tsDyn'*. Available from: `http://cran.r-project.org`.
62. R. J. Hyndman, G. Athanasopoulos, C. Bergmeir, G. Caceres, L. Chhay, M. O'Hara-Wild, et al., *Package 'forecast'*, 2026. Available from: `https://cran.r-project.org/web/packages/forecast/forecast.pdf`.
63. T. Hayfield, J. S. Racine, Nonparametric econometrics: The np package, *J. Stat. Softw.*, **27** (2008), 1–32. https://doi.org/10.18637/jss.v027.i05
64. F. X. Diebold, Comparing predictive accuracy, twenty years later: A personal perspective on the use and abuse of Diebold–Mariano tests, *J. Bus. Econ. Stat.*, **33** (2015). https://doi.org/10.1080/07350015.2014.983236
65. H. Iftikhar, F. Khan, E. A. Torres Armas, P. C. Rodrigues, J. L. López-Gonzales, A novel hybrid framework for forecasting stock indices based on the nonlinear time series models, *Comput. Stat.*, **40** (2025), 4163–4186. https://doi.org/10.1007/s00180-025-01614-5
66. H. Iftikhar, M. Khan, J. E. Turpo-Chaparro, P. C. Rodrigues, J. L. López-Gonzales, Forecasting stock prices using a novel filtering-combination technique: Application to the pakistan stock exchange, *AIMS Math.*, **9** (2024), 3264. https://doi.org/10.3934/math.2024159
67. H. Iftikhar, A. Zafar, J. E. Turpo-Chaparro, P. Canas Rodrigues, J. L. López-Gonzales, Forecasting day-ahead brent crude oil prices using hybrid combinations of time series models, *Mathematics*, **11** (2023), 3548. https://doi.org/10.3390/math11163548
68. H. Iftikhar, M. Qureshi, P. C. Rodrigues, M. U. Iftikhar, J. L. López-Gonzales, Daily crude oil prices forecasting using a novel hybrid time series technique, *IEEE Access*, **13** (2025), 98822–98836. https://doi.org/10.1109/ACCESS.2025.3574788